AKADÉMIAI KIADÓ

Central European Geology

64 (2021) 1, 38–58

DOI:
10.1556/24.2021.00005

ORIGINAL RESEARCH PAPER

Tourmalines of the Velence Granite Formation and the surrounding contact slate, Velence Mountains, Hungary

BÉLA FEHÉR[1] and NORBERT ZAJZON[2*]

[1] Department of Mineralogy, Herman Ottó Museum, Miskolc, Hungary

[2] Institute of Mineralogy and Geology, University of Miskolc, Miskolc, Hungary

Received: October 14, 2020 • Accepted: March 02, 2021
Published online: April 2, 2021

ABSTRACT

Three distinct paragenetic and compositional types of tourmaline were described from the Velence Granite and the surrounding contact slate. Rare, pitch-black, disseminated tourmaline I (intragranitic tourmaline) occurs in granite, pegmatite, and aplite; very rare, black to greenish-gray, euhedral tourmaline II (miarolitic tourmaline) occurs in miarolitic cavities of the pegmatites; abundant, black to gray, brown to yellow or even colorless, acicular tourmaline III (metasomatic tourmaline) occurs in the contact slate and its quartz-tourmaline veins. Tourmaline from a variety of environments exhibits considerable variation in composition, which is controlled by the nature of the host rock and the formation processes. However, in similar geologic situations, the composition of tourmaline can be rather uniform, even between relatively distant localities. Tourmaline I is represented by an Al-deficient, Fe^{3+}-bearing schorl, which crystallized in a closed melt-aqueous fluid system. Tourmaline II is a schorl-elbaite mixed crystal, which precipitated from Li- and F-enriched solutions in the cavities of pegmatites. Tourmaline III shows an oscillatory zoning; its composition corresponds to schorl, dravite, and foitite species. It formed from metasomatizing fluids derived from the granite. This is the most abundant tourmaline type, which can be found in the contact slate around the granite.

KEYWORDS

contact slate, crystal chemistry, electron-microprobe analyses, tourmaline, Velence Granite Formation, Hungary

INTRODUCTION

Tourmaline is the most common borosilicate mineral and the most important reservoir of boron in granitic systems. It appears in peraluminous granites, pegmatites, and aplites as a dispersed accessory phase, within miarolitic cavities, and as a metasomatic phase in the adjacent wall rocks (London, 1999). Its chemical composition depends on the origin and evolution of the parental magma or fluid phases (Henry and Guidotti, 1985). Tourmaline may have crystallized during the early magmatic evolution of granitic rocks, through early subsolidus to hydrothermal conditions (London and Manning, 1995).

Tourmaline is known for more than a century in the contact slate of the Velence Mountains (Vendl, 1914). However, Vendl (1914) did not assume any connection between the tourmalinization of the contact slate and the granite, as no tourmaline was found in the granite itself. According to him, tourmaline had already occurred in the original, uncontacted slate. Some years later his sister described the first intragranitic tourmaline from an aplite mine opened during World War I, located at Kisfaludy Farm, near Székesfehérvár (Vendl, 1923). In his work on the geology of the Velence Mountains, Jantsky (1957) mentioned several tourmaline occurrences, but he did not carry out any detailed studies on the mineral. He considered all the tourmalines in the mountains to be of pneumatolytic origin. In the latest work on the geology of the Velence Mountains, tourmaline is only mentioned in a few

*Corresponding author. Institute of Mineralogy and Geology, University of Miskolc, 3515 Miskolc-Egyetemváros, Hungary.
E-mail: nzajzon@uni-miskolc.hu

AKJournals

paragraphs (Gyalog and Horváth, 2004). Until now, chemical analyses of the Velence tourmaline have not been published.

In this paper the first crystal chemical data of the Velence tourmalines are published; the morphological, textural and paragenetic types of tourmaline are also described, with presentation of their formation in magmatic versus hydrothermal stage and in closed versus open system.

GEOLOGIC SETTING

The main mass of the Velence Mountains is made up of Permian biotitic monzogranite (Fig. 1). The mountains are bordered by Lake Velence to the southeast and south, while to the northwest, the Csákvár Depression separates it from the Vértes Mountains. To the north it is bordered by the Lovasberény region, consisting of loess and Pannonian formations (Vendl, 1914). Reported radiometric ages of the granite magmatism scatter between 271 and 291 Ma (Buda et al., 2004b); the most reliable zircon U–Pb age is 282 ± 3 Ma (Uher & Ondrejka, 2009), which corresponds to the Early Permian, unlike the earlier conceptions that place the Velence Granite Formation into the Carboniferous (see e.g., Jantsky, 1957; Gyalog and Horváth, 2004).

The granite and its vein rocks of the Velence Mountains are classified as the Velence Granite Formation (Gyalog and Horváth, 2004). Vendl (1914) was still uncertain whether the granite body was a laccolith or batholite. Gyalog and Horváth (2004) clearly speak of granite batholite, the formation of which was divided into three phases. The first (early) crystallization phase is represented by the rounded decimeter-size, microdioritic–granodioritic xenoliths. In the second (main) phase, the biotite granite itself was formed at a hypabyssal depth (3–7 km). In the late stage of the main crystallization, the dike-like, true (or dilatation) aplite and

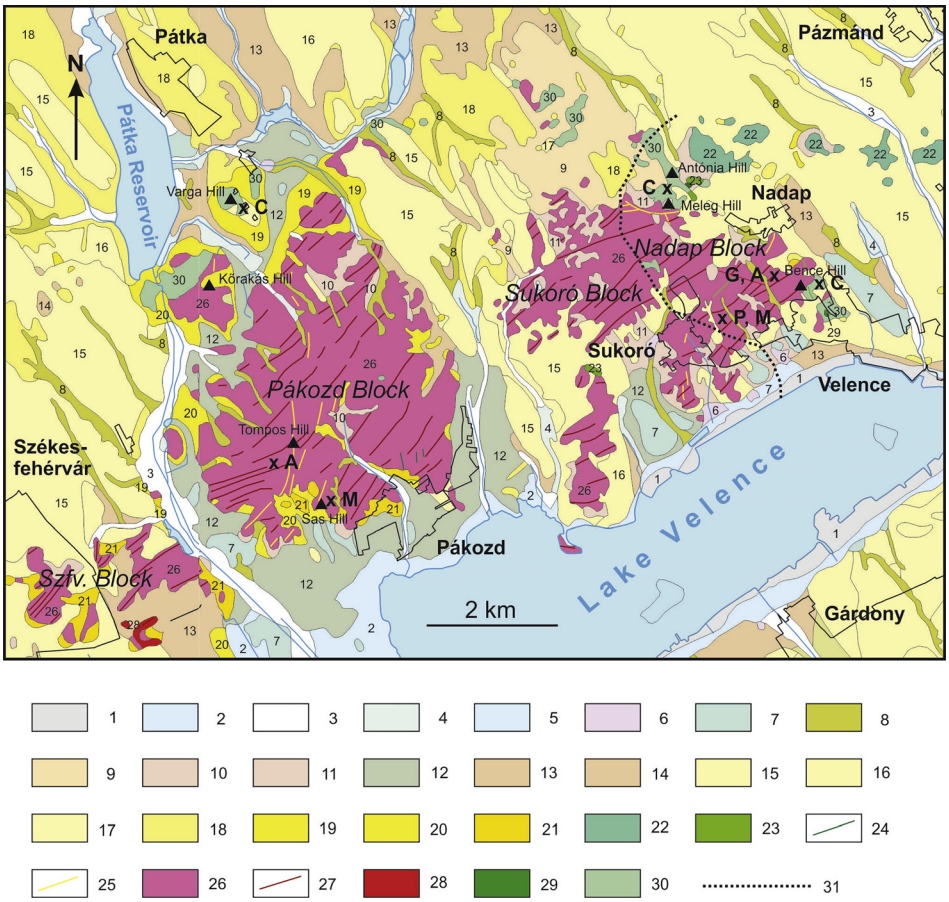

Fig. 1. Geologic map of the Velence Mountains (after Gyalog, 2005a, b) with the sampling sites. Legend: 1 = artificial filling up; 2–17 = Pleistocene and Holocene formations; 18 = Upper Pannonian Tihany Formation; 19 = Upper Pannonian Tihany and Kálla Formations (merged); 20 = Upper Pannonian Kálla Gravel Formation; 21 = Pannonian talus; 22 = Middle-Upper Eocene Pázmánd Metasomatite Member of the Nadap Andesite Formation; 23 = Middle-Upper Eocene Sorompóvölgy Andesite Member of the Nadap Andesite Formation; 24 = Upper Cretaceous Budakeszi Picrite Formation; 25 = Cretaceous quartz vein; 26 = Lower Permian Velence Granite Formation; 27 = Lower Permian Pákozd Granite Porphyry Member of the Velence Granite Formation; 28 = Lower Permian Kisfalud Microgranite Member of the Velence Granite Formation; 29 = Silurian-Devonian Bencehegy Microgabbro Formation; 30 = Ordovician-Devonian Lovas Slate Formation; 31 = western border of the fluid infiltration connected with the Eocene andesitic volcanism (after Benkó et al., 2014). The collecting sites of the examined tourmaline samples are marked with x, indicating the type of host rock (A = aplite; C = contact slate or quartz-tourmaline vein; G = granite; M = miarolitic cavity; P = pegmatite). Abbreviation: Szfv. Block = Székesfehérvár Block

small pegmatite nests were formed as the products of magmatic differentiation. Finally, in the third (so-called dike-forming) stage, the granite was cross-cut by dike swarms of different ages, including granular aplite, silicified intrusive breccia, microgranite, and granite porphyry dikes. The latter are placed stratigraphically into the Pákozd Granite Porphyry Member; two known types are the older ("Sukoró") type, which formed even before the granite had cooled down, and the younger ("Pátka") type, which intruded into the cracks of the by then lower-temperature batholite (Embey-Isztin, 1974, 1975). Tourmaline formation is not related to the rocks of the early phase.

The Velence Granite was intruded into the Early Paleozoic Lovas Slate Formation, the initial rocks of which were clayey, silty, and sandy sediments containing tuffs in some levels (Gyalog and Horváth, 2004). The granite itself was intruded into a slate that had already undergone folding and low-grade regional metamorphism. A wide contact zone developed in the slate around the granite. Vendl (1914) distinguished two types of these contact metamorphic rocks: the first is an andalusite-bearing hornfels that had metamorphized at higher temperature (hornblende hornfels facies), and the second is the so-called knotted slate with lower temperature metamorphism (albite-epidote hornfels facies). These contact rocks covered the surface of the granite everywhere during the granite magmatism, but today only their shreds remain on the northern and eastern sides of the granite area (Fig. 1, Formation 30). In the Velence Mountains, the most abundant appearance of tourmaline is associated with the knotted slate. Tourmaline in the slate appears in tiny black knots or veinlets, but in some places (Varga and Antónia Hills), the slate has been converted into tourmaline-fels. Vendl (1914) had not yet tied the tourmalinization of the contact slate to the granite, as no tourmaline had been found in the granite itself, so he thought the tourmaline had already appeared in the original, uncontacted slate.

Benkó et al. (2014) suggested that the quartz-fluorite-base metal veins and the clayey (illite, kaolinite, smectite) transformation zones around them, observed in several places in the granite, are products of Middle or Late Triassic hydrothermal activity, based on K/Ar radiometric age-dating carried out on vein-filling illite. Triassic magmatic rocks are not found in the Velence Mountains; since they are only known in the nearby Szabadbattyán Block (andesite dikes in a Devonian limestone), Benkó et al. (2014) considered these hydrothermal fluids to be unrelated to magmatic activity.

The rocks of the Upper Cretaceous magmatism are classified into the Budakeszi Picrite Formation (Fig. 1, Formation 24). They appear as dikes in the granite and represent three types of rocks: spessartite, monchiquite, and beforsite. Based on the REE content of fluorite, the formation of the above-mentioned quartz-fluorite-base metal veins is linked to this Cretaceous magmatism by Horváth et al. (1989).

The rocks associated with Eocene andesite volcanism are located in the eastern part of the mountains (Fig. 1, Formations 22 and 23) and belong to the Nadap Andesite Formation (Gyalog and Horváth, 2004). Its rocks also appear as minor subvolcanic bodies in the granite and the contact slate. Fluid flows associated with Paleogene volcanism are limited in space to the Eocene volcanic unit and to the easternmost part of the granitic area (Benkó et al., 2014). The western boundary of the Paleogene fluid flow in granite is shown by a dotted line in Fig. 1.

MINERALOGICAL AND PETROGRAPHIC DESCRIPTION OF THE GRANITE AND ITS VEIN ROCKS

Vendl (1914) had already reported in detail on the petrographic conditions of the Velence Granite. He found that the main rock-forming minerals of the granite are pink orthoclase, white plagioclase, gray quartz, and brownish-black biotite. Among the accessory minerals he mentioned apatite, zircon, epidote, and pyrite.

On the basis of modal analyses, according to the IUGS classification, the Velence granitoids are mostly monzogranites, with lesser granodiorites, and some samples represent alkaline-feldspar granites. Increased SiO_2 and K_2O contents and relatively reduced contents of Al_2O_3, MgO, CaO, and P_2O_5 are characteristic of the chemical composition of the Velence granitoids. On the other hand, the contents of alkalis are slightly increased. The granitoids are slightly peraluminous or even metaluminous (A/CNK = 0.96–1.37, see Fig. 2) and they display a trend to post-orogenic granites (Uher and Broska, 1994).

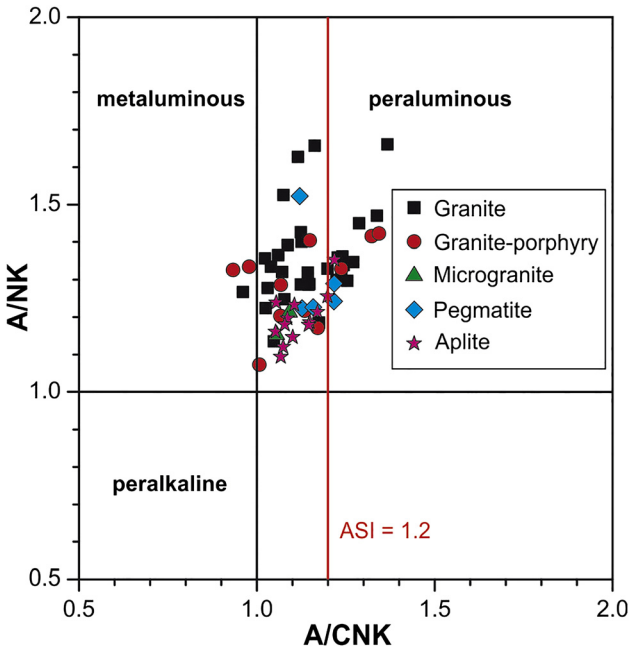

Fig. 2. Compositions of the Velence Granite and its vein rocks plotted in the A/CNK vs. A/NK discriminating diagram (Maniar and Piccoli, 1989). A = Al_2O_3, C = CaO, N = Na_2O and K = K_2O in mol%. Data sources: Jantsky (1957), Nagy (1967a), Pantó (1977), Buda (1993), Uher and Broska (1994) and Gyalog and Horváth (2004). ASI = alumina saturation index

Texturally two types of granite are distinguished: a medium to coarse-grained, slightly porphyritic or equigranular biotitic granite, and a fine-grained porphyritic granite, which is enriched in biotite (Gyalog and Horváth, 2004).

The average modal composition of granite is 34% quartz, 28% potassium feldspar, 31% plagioclase, and 6% mafic minerals. The magmatic body has been crystallized from an eutectic melt, saturated with volatiles, approximately at 2 kbar pressure (Buda, 1985). The Velence granitoids are characterized by qualitatively (in terms of the number of determined mineral phases = ca. 30; see Szakáll et al., 2016) as well as quantitatively (180–1,180 ppm) poor accessory mineral assemblages, with zircon and apatite as the most frequently occurring minerals (Uher and Broska, 1994).

Although the granite of the Velence Mountains has long been classified as S-type (e.g., Buda, 1985), in the present study the classification of Uher and Broska (1996) is applied, who stated that the Velence granite is a typical subsolvus, post-orogenic, post-collisional, felsic plutonic suite with mildly A-type character.

The feldspars of the granite were studied in detail by Buda (1969, 1974). He distinguished two types of potassium feldspar: perthite-free and fine perthitic feldspar. On the basis of X-ray examinations, they are structurally almost always monoclinic, i.e., orthoclase. Both its optical properties (intermediate 2V, i.e., the so-called intermediate orthoclase) and its chemical composition (average: Or = 70.2, Ab = 27.7, An = 2.1 mol%) indicate high formation temperatures and relatively rapid cooling rates. The temperature of the formation of potassium feldspar is 600–680 °C according to Buda (1969, 1981, 1993).

The most common type of plagioclase is twinned, slightly sericitized crystals, but there are also zonal plagioclases, as well as perthitic exsolution forms in potassium feldspar. The first type has an Ab = 70 and An = 30 mol% composition, with an average formation temperature of 520 °C, so they formed after the potassium feldspar (Buda, 1969).

The shape of quartz is mostly anhedral. Its color is macroscopically gray, and colorless in thin section. The quartz grains are highly cracked and often have an undulatory extinction (Nagy, 1967b). From the morphology, Buda (1969) concluded that quartz could be formed at temperatures above 573 °C.

The fresh biotite is brownish-black in color, sometimes reaching 0.5 cm in size. The composition of the mineral varies from site to site (Nagy, 1967b). Generally, the high $Fe_{tot}/(Fe_{tot} + Mg)$ ratio (0.68–0.93) is characteristic for the biotite (i.e., all biotite corresponds to annite), which is a good reflection of the low Mg content of the granitic melt.

Rare pegmatites occur in two forms: lenticular and nest-like, rounded-elongated bodies (up to 1–2 m^3). The structure of the lenticular pegmatitic bodies is quite simple. Generally, their marginal zones are fine-grained, followed by coarse-grained, graphic-textured zones of quartz and K-feldspar. The central parts of these lenses are filled with subhedral or anhedral quartz crystals, or less frequently by K-feldspar. Plagioclase and biotite occur in subordinate amounts in these lenses (Molnár et al. 1995). The formation temperature of the pegmatites is about 500–600 °C (Buda 1969, 1993; Molnár et al. 1995). The Velence pegmatites were classified into the NYF family on the basis of the heavy rare earth elements, uranium and thorium enrichment, the Nb > Ta relation, the frequency of allanite-(Ce), keralite and xenotime-(Y), the presence of gadolinite-(Y), and the absence or minimal amount of tourmaline (Wise, 1999; Szakáll et al., 2014; Zajzon et al., 2015).

Embey-Isztin (1974, 1975) dealt with the petrographic relations of the aplites in detail, two types of which were distinguished: 1.) dilatation-injection-type aplite; 2.) replacement aplite. These two types correspond to Vendl's (1914) porphyry and granular aplite, respectively. The dilatation-injection (porphyry) aplite always forms veins with a thickness of 1–10 m and a length of up to a few 100 m. Similarly to granite-porphyry dikes, they formed by dilation and melt impregnation. Replacement (granular) aplite may also form veins, as well as nests and stocks. These were created in the subsolidus period of granite genesis by displacement, autometamorphic, and autometasomatic processes, without dilatation. Tourmaline formation is linked to the latter (granular) aplite.

The tiny miarolitic cavities are up to 0.001 m^3, characterized by the presence of euhedral quartz (in some places smoky quartz or amethyst), K-feldspar and albite. Rarely biotite or tourmaline and garnet can also be observed. Mineral formation temperatures range from 310 to 400 °C (Molnár et al. 1995).

The characterization of granite-porphyry dikes was not considered, because tourmaline formation is not linked to them.

ANALYTICAL METHODS AND CALCULATING PROCEDURES

The composition of tourmaline was established with a JEOL JXA-8600 electron microprobe (upgraded by SAMX control) in wavelength-dispersive mode (WDX) at the University of Miskolc, Miskolc, Hungary. The analytical conditions were: accelerating voltage 15 kV, beam current 20 nA, and beam diameter of 1–5 μm. The tourmaline samples were analyzed with the following standards: quartz (Si), ilmenite (Ti and Fe), corundum (Al), MnS_2 (Mn), olivine (Mg), Cr-augite (Ca), gahnite (Zn), anorthoclase (Na), microcline (K), and LiF (F). The peak and background count times were 10 and 5 s, respectively for all the analyzed elements except for fluorine (30 and 15 s, respectively). The analytical data were normalized according to the PAP procedure (Pouchou and Pichoir, 1985).

The crystal chemical formulas of tourmaline were calculated on the basis of 31 O + OH + F anions according to the general formula $XY_3Z_6T_6O_{18}(BO_3)_3V_3W$, with the most common constituents being: $^{[9]}X = Na^{1+}, Ca^{2+}, K^{1+}$, vacancies ([]); $^{[6]}Y = Fe^{2+}, Mg^{2+}, Mn^{2+}, Al^{3+}, Li^{1+}, Fe^{3+}, Cr^{3+}$; $^{[6]}Z = Al^{3+}, Fe^{3+}, Mg^{2+}, Cr^{3+}$; $^{[4]}T = Si^{4+}, Al^{3+}$; $^{[3]}B = B^{3+}$; $V = OH^{1-}, O^{2-}$; $W = OH^{1-}, F^{1-}, O^{2-}$

(Henry et al., 2011). When the total cation contents of the T + Z + Y sites exceeded 15 apfu, some ferric iron contents were assumed. In this case the FeO/Fe_2O_3 ratio was calculated to satisfy the T + Z + Y = 15 apfu equation. This approximation provides the estimated values of minimal ferric iron content, where we do not count for the presence of lithium or vacancies in the Y-site and oxygen in the V- and W-sites.

Boron was assumed to be present with a value of 3 apfu, because crystal structure refinements and bond valence calculations indicate that there are essentially 3 B apfu in those tourmalines that have been determined to date (Hawthorne, 1996). Tourmalines in miarolitic cavities of granite pegmatites may contain a significant amount of lithium at the Y-site. In such cases, the Li content of tourmaline can be calculated stoichiometrically by initially normalizing to 29 oxygens basis, and then estimating Li content by the expression Li = 3 – ΣY (in apfu) (Henry and Dutrow, 1996).

Site occupancies were calculated assuming that Si deficiency in the tetrahedral site (T) is compensated by Al. Consequently, if Al < 6 apfu, Mg and Fe^{3+} compensate Z-site occupancy, while Y-site is filled by the remaining Al, Mg, Mn, Fe^{2+}, Fe^{3+}, and Ti cations. The X-site is occupied by Na, Ca or may be vacant. Ordered cation distribution was assumed, so disordering of Al, Mg, and Fe at the two octahedrally coordinated sites (Y and Z) was not considered (for the details of cation ordering-disordering in tourmaline see e.g., Grice and Ercit, 1993; Bačík, 2015).

THE TOURMALINES

Tourmaline types and samples

Tourmaline occurs in three distinct paragenetic and morphological types in macroscopic scale. Tourmaline I or intragranitic tourmaline: pitch black, disseminated, stubby columnar crystals up to 2 cm in length. It is a rare accessory phase in the granite and some pegmatites and aplites. Tourmaline II or miarolitic tourmaline: black, greenish-black, greyish-green, grown-up, euhedral, stubby columnar crystals up to 4 mm in length in miarolitic cavities. It is very rare in the Velence Mountains. Tourmaline III or metasomatic tourmaline: black, gray, greyish-brown, or even colorless, long prismatic or acicular crystals up to 15 mm in length in fine-grained or fibrous aggregates (Fig. 3). It is the most common tourmaline type in the Velence Mountains, which occurs in the contact slate surrounding the granite body, or in quartz-tourmaline veins. Tourmaline III can accumulate locally in larger quantities forming tourmaline-fels (Varga Hill, Pátka; Antónia Hill, Lovasberény).

In the *granite* itself, tourmaline can be found extremely rarely, only in small quantities. Only one tourmaline sample of the granite could be examined from Bence Hill, Velence (Table 1). The sample was collected by Béla Jantsky in the 1950s and found in the collection of the Mining and Geological Survey of Hungary (MBFSZ, formerly Geological Institute of Hungary, Budapest) under catalog number 5307. Generally, here the tourmaline forms pitch black crystals up to 2 cm. On the BSE image the mineral shows no chemical zoning.

The mineralogy of the *pegmatites* is extremely simple, because basically only the three main rock-forming minerals of the granite (i.e., quartz, K-feldspar, and minor biotite) build them. The Velence pegmatites are rather poor in accessory minerals, so they contain tourmaline occasionally. In the present study, we were able to examine only one of the pegmatite sites found in the former rubblestone mine at Sukoró, where tourmaline-bearing samples were collected by Béla Nagy in 1965 and 1974. The three samples examined can be found in the collection of the MBFSZ under the catalog numbers 11138, 11144, and 11149 (Table 1).

The tourmaline-containing pegmatite of Sukoró was described in detail by Nagy (1967a). According to his study, the pegmatite formation is linked to a biotitic aplite dike in which lens-shaped pegmatitic formations have been developed in an asymmetric arrangement (Fig. 4). Their dimensions depend on the thickness of the aplite dike. Their main minerals are quartz, K-feldspar, plagioclase (albite to andesine composition), biotite, and amphibole. The tested tourmaline forms pitch black, stubby columnar crystals with triangular cross-section, that can reach 1.5–2 cm in length, and came from the formation No. 5 of Fig. 4. The crystals are fragmented, their cracks filled with quartz and kaolinized feldspar.

From the *aplites* two tourmaline samples were examined. One of them is a black tourmaline from the Bence Hill in Velence, which was collected by Béla Jantsky in 1951 and found in the collection of the MBFSZ under catalog number 5304. Here, tourmaline forms a black-colored veinlet (see Fig. 26 of Jantsky, 1957). The other sample comes from the aplite of Tompos Hill in Pákozd, which was collected by Sándor Szakáll in 2014 (V3 sample, Table 1). The host rock is a light-colored aplite, which consists of quartz, perthitic K-feldspar, and albite in addition to the tourmaline. The composition of the potassium feldspar is $Or_{86.3–96.8}Ab_{3.0–12.6}An_{0.1–1.1}$, while that of the albite is $Or_{1.0–1.3}Ab_{95.3–98.5}An_{0.3–3.5}$. Tourmaline forms black, subhedral, or euhedral crystals typically below mm-size. Some potassium feldspars contain shred-like fragments of tourmaline, which have the same composition as the adjacent tourmaline. Interestingly, the aplite dike passes through a coarse-grained pegmatite, in which no tourmaline was observed.

The mineral association of the miarolitic cavities is very similar to that of the pegmatites; their main component is quartz, the columnar crystals of which can exceed 10 cm in length. They often represent the smoky quartz variety. Another common component is the pink K-feldspar, which can form several centimeter-sized, euhedral, stubby columnar crystals, and represents the orthoclase mineral species. Rarely, colorless plagioclase, and platy muscovite or biotite also appear. Two tourmaline-bearing samples were investigated: one from Sas Hill in Pákozd, and the other from the rubblestone mine of Sukoró (Table 1).

The tourmaline of Sas Hill was collected by László Kupi in November 2007. The specimen was derived from a small

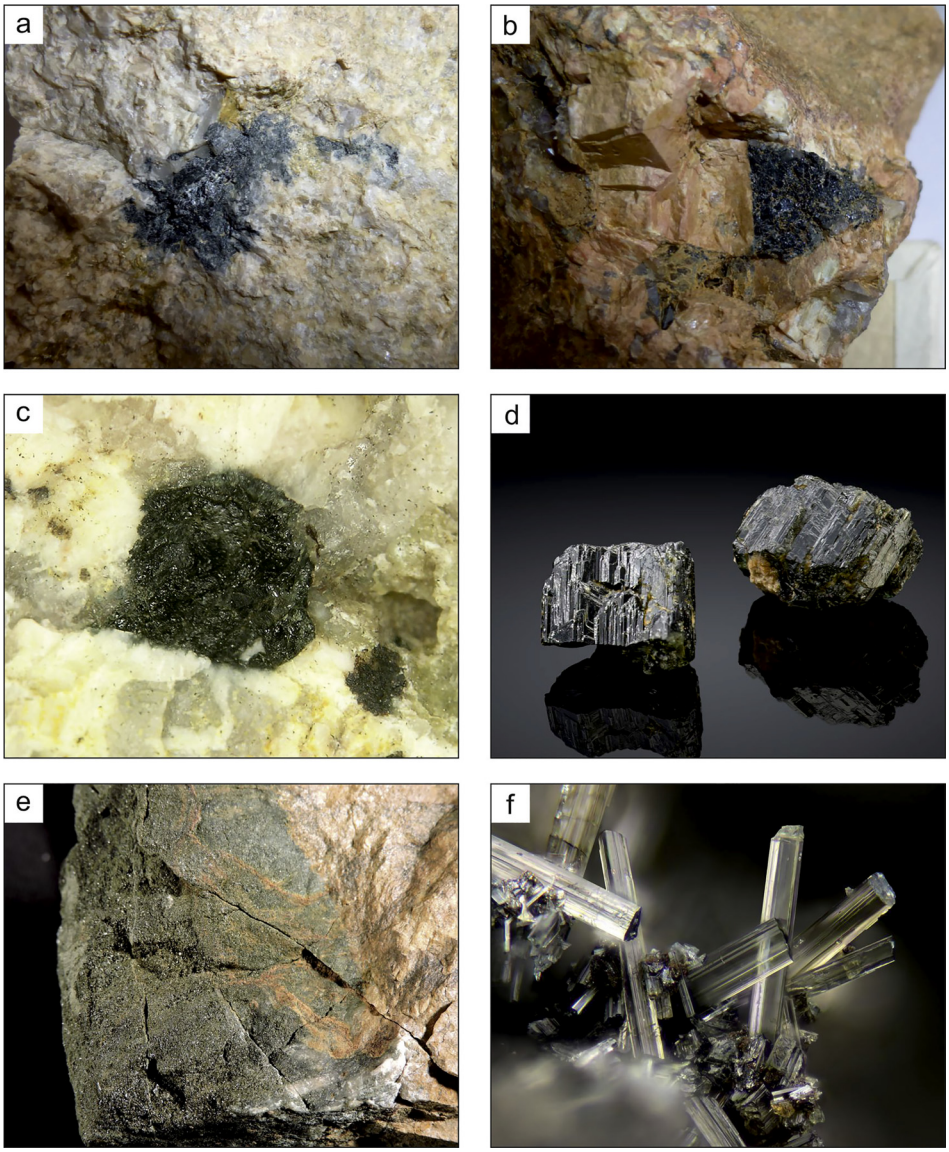

Fig. 3. a.) Tourmaline I in granite, Bence Hill, Velence (MBFSZ-5307). FOV: 6 cm. Photo: Bálint Péterdi. b.) Tourmaline I in pegmatite, rubblestone mine of Sukoró (MBFSZ-11144). FOV: 6 cm. Photo: Bálint Péterdi. c.) Tourmaline I in aplite, Tompos Hill, Pákozd (V3). FOV: 7 mm. Photo: Béla Fehér. d.) Tourmaline II from a miarolitic cavity, Sas Hill, Pákozd (HOM-2009.215). FOV: 8 mm. Photo: László Kupi. e.) Tourmalinized contact slate with tourmaline III, Varga Hill, Pátka (HOM-26284). FOV: 6 cm. Photo: Béla Fehér. f.) Colorless, columnar tourmaline III in contact slate, Varga Hill, Pátka (not analyzed). FOV: 1.5 mm. Collection and photo: László Tóth

miarolitic cavity near an aplite veinlet when a sewage pipeline of a building was laid. The site was collectible only for a few days. It is interesting to note that it also contained green feldspar besides the tourmaline (oral communication by László Kupi). The tourmaline forms 2 to 4 mm, black, stubby columnar crystals, which turns green at their thin edges towards the light. Some crystal faces can be observed on them. The investigated specimen can be found in the mineral collection of Herman Ottó Museum, Miskolc (HOM, catalog No. 2009.215).

The Sukoró sample is a "green" tourmaline, which was described as elbaite by Nagy (1967a) from a miarolitic cavity of the pegmatite (see Fig. 4, No. 3). The tested specimen was collected by Béla Nagy in March 1974 in the rubblestone quarry of Sukoró and now it is in the collection of the MBFSZ under the catalog number 11133.

Originally, the granite batholite was completely covered by the contact slate, but today only a few remains of the slate can be observed on the surface at some sites (e.g., Bence, Antónia, and Varga Hills; see formation No. 30 on Fig. 1). While the aforementioned genetic types caused problems with the limited number of samples, the tourmalines of the contact slate and quartz veins were available to study in large numbers. This is not surprising, since the volume of tourmaline formation associated with the Velence Granite was significant not within the granite body but within the contact zone around it. Eight samples have been subjected to crystal-chemical investigation, as listed in Table 1.

Table 1. List of the studied samples

Sample	Type*	Locality	Rock type
MBFSZ-5307	I	Bence Hill, Velence	Granite
MBFSZ-11138	I	Sukoró	Pegmatite
MBFSZ-11144	I	Sukoró	Pegmatite
MBFSZ-11149	I	Sukoró	Pegmatite
MBFSZ-5304	I	Bence Hill, Velence	Aplite
V3	I	Tompos Hill, Pákozd	Aplite
HOM-2009.215	II	Sas Hill, Pákozd	Miarolitic cavity in pegmatite
MBFSZ-11133	II	Sukoró	Miarolitic cavity in pegmatite
MBFSZ-5301	III	Bence Hill, Velence	Brecciated quartz-tourmaline vein
MBFSZ-5297	III	Antónia Hill, Lovasberény	Quartz-tourmaline vein
HOM-18142	III	Antónia Hill, Lovasberény	Quartz-tourmaline vein
HOM-17701	III	Antónia Hill, Lovasberény	Quartz-tourmaline vein
HOM-25922	III	Antónia Hill, Lovasberény	Quartz-tourmaline vein
HOM-23596	III	Varga Hill, Pátka	Quartz-tourmaline vein
HOM-26284	III	Varga Hill, Pátka	Contact slate
V1	III	Varga Hill, Pátka	Contact slate ("tourmaline fels")

* Tourmaline types: I: intragranitic, II: miarolitic, III: metasomatic.

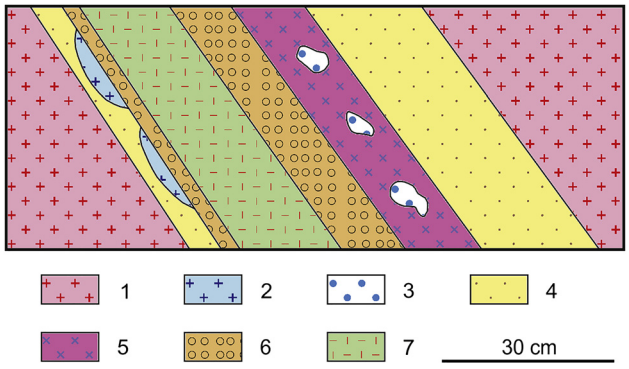

Fig. 4. Simplified section of the tourmaline-bearing pegmatite from Sukoró (after Nagy, 1967a). Legend: 1 = granite; 2 = graphic granite; 3 = miarolitic cavity; 4 = microgranite; 5 = tourmaline-bearing graphic granite; 6 = coarse-grained pegmatite; 7 = aplite

The tourmaline associated with the contact slate and quartz veins has a slightly lighter macroscopic color than tourmaline in the granite and its vein rocks, i.e., it is not particularly black, but rather dark gray, gray, sometimes brown, yellow, or even colorless. The crystals are usually elongated columnar or fibrous in habit, but in some quartz veins they form massive, fine-grained aggregates, where individual crystallites often cannot be separated even under a binocular microscope, so that they are less than 0.1 mm in size. Other times, however, the acicular crystals may be up to 1.5 cm in length.

The locations of all the investigated samples are shown in Fig. 1.

Chemical composition

Intragranitic tourmaline (tourmaline I). The chemistry of the tourmalines in the granite, the pegmatite and the aplite are essentially the same, so they are discussed together as intragranitic tourmaline. These tourmalines occur as disseminated crystals or veinlets and are characterized by lack of chemical zoning, not counting the reaction rims observed on some pegmatitic crystals (e.g., the sample MBFSZ-11138) (Fig. 5a–c).

Representative chemical analyses of tourmaline I are given in Table 2. At the X-site, alkali metals predominate, since the Na content varies between 0.71 and 0.98 apfu. Thus, this tourmaline belongs to the alkali group (Fig. 6). The amount of Ca is not significant (up to 0.11 apfu) and the number of vacancies is rather low (0–0.21 apfu). The tourmaline I exhibits 5.79 to 6.03 apfu Si in the T-site, so the ^{T}Al-content varies between 0 and 0.21 apfu. These disseminated tourmalines are characterized by a low total Al-content (5.43–6.11 apfu); therefore, Al usually cannot fully occupy the Z-site (^{Z}Al = 5.34 to 6.00 apfu). Hence some Mg and Fe (mainly ferric iron) enter to this position. The most diverse cation occupation can be observed in the Y-site, where Fe^{2+} is dominant (2.54–2.89 apfu). Due to the low total Al content, Al cannot be incorporated here; also, the Mg, Mn, and Ti are insignificant, while Fe^{3+} can be present in a more elevated amount (up to 0.34 apfu). Fluorine was not detected at the W-position, so OH was always counted as 1 apfu. Therefore, this tourmaline is a member of the hydroxy series, although no data are available on the extent of any oxygen substitution. Since oxygen can be incorporated into the W-site of schorl by the $^{Y}Fe^{2+} + {}^{W}(OH)^{-} = {}^{Y}Fe^{3+} + {}^{W}O^{2-}$ substitution and the calculated iron content of the intragranitic tourmaline is high, no significant O content can be expected in this structural position (Table 2).

Based on the crystal-chemistry discussed above, intragranitic tourmaline (tourmaline I) represents the schorl mineral species, which does not show transition toward dravite due to the lack of Mg at the Y-site. It rather forms a transition to foitite owing to some vacancies at the X-site (Fig. 7), and it contains some povondraite components because of the calculated ferric iron content.

Reaction rims appeared at the edge of some tourmaline grains of the MBFSZ-11138 sample, which are very thin (up

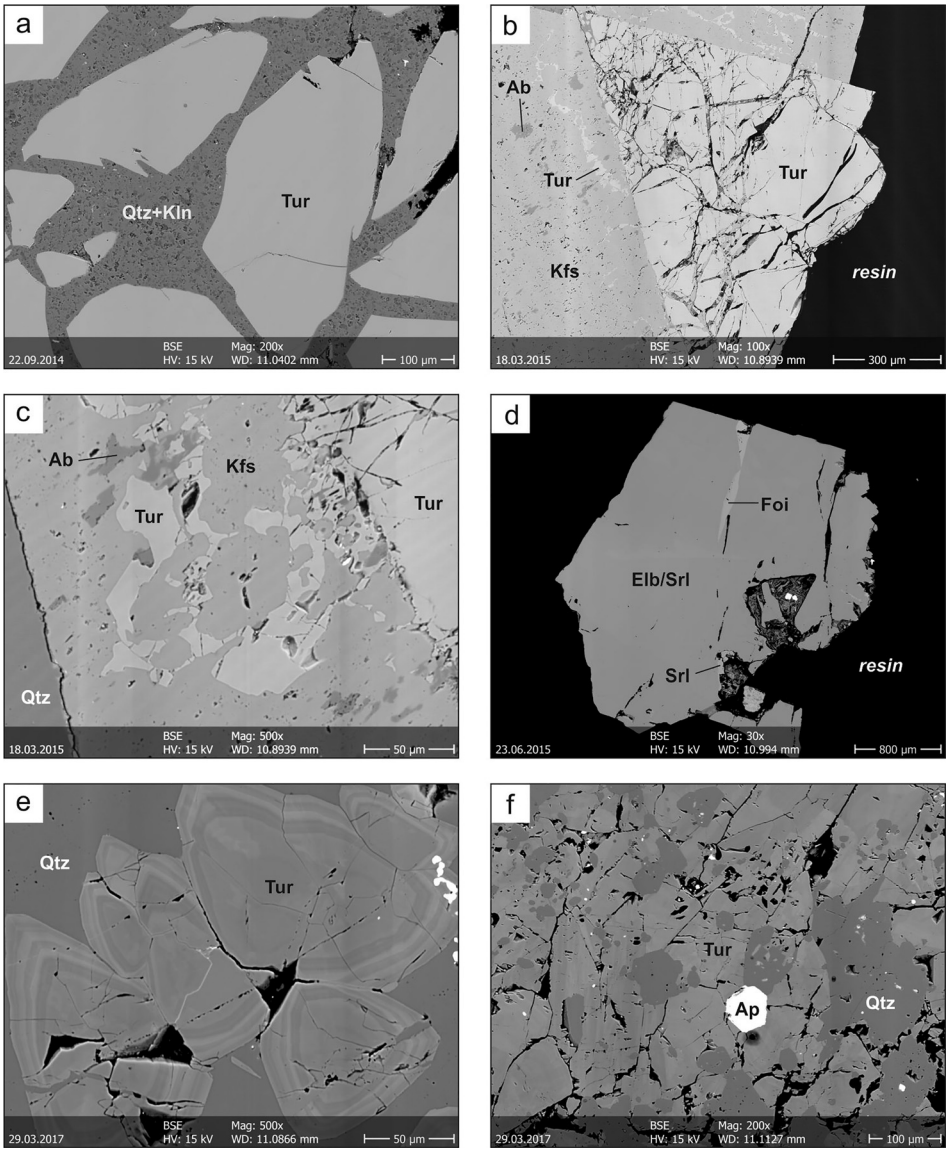

Fig. 5. BSE images of tourmaline samples. a.) Unzoned tourmaline I fragments with quartz and kaolinized K-feldspar from the Sukoró pegmatite (sample MBFSZ-11144); b.) Unzoned, euhedral, cracked tourmaline I from aplite of Tompos Hill, Pákozd (sample V3); c.) Partly tourmalinized K-feldspar in the sample V3; d.) Euhedral, chemically (dominantly) homogeneous elbaite-schorl mixed crystal (tourmaline II) from a miarolitic cavity of a pegmatite from Sas Hill, Pákozd (sample HOM-2009.215) with a foititic alteration zone and a minute schorl rim; e.) Euhedral tourmaline III showing oscillatory zoning from a quartz-tourmaline vein of Varga Hill, Pátka (sample HOM-23596); f.) Zoned tourmaline III partially consumed by quartz from a quartz-tourmaline vein of Antónia Hill, Lovasberény (sample HOM-17701). Abbreviations: Ab = albite, Ap = apatite, Elb = elbaite, Foi = foitite, Kfs = K-feldspar, Kln = kaolinite, Qtz = quartz, Srl = schorl, Tur = tourmaline

to 3 µm thick); thus, accurate WDX analyzes could not be made. In order to get some information of the substitution trends in the rim relative to the main mass of the crystals, some EDX analyses were made with a focused electron beam. Unfortunately, the excitation volume exceeded the measured phase, as the amount of Si in the formula calculated for the 31 anions was significantly higher than the ideal value of 6 apfu. This surplus Si most probably came from the surrounding quartz. For this reason, this surplus Si was extracted from the analyses and the formulas calculated so that 6 apfu Si was placed at the T-site. The measurements were not tabulated because of their high uncertainty; the composition calculated from one analysis is as follows:

$([]_{0.56}Na_{0.42}Ca_{0.02})_{\Sigma=1.00}$ $(Fe^{2+}{}_{1.80}Al_{0.64}Mg_{0.49}Ti_{0.01}Mn_{0.01})_{\Sigma=2.95}$ $Al_{6.00}$ $Si_{6.00}$ O_{18} $(BO_3)_3$ $(OH)_4$, which corresponds to the foitite mineral species. This tourmaline is considered to be the transformation product of the pegmatitic tourmaline, which could have been generated by the fluid infiltration after pegmatite formation. The infiltrating fluid itself can be a product of the Paleogenic volcanism, as the site of the sample falls into the fluid flow zone of the Eocene andesite volcanism (see Fig. 1). The fact

Table 2. Representative electron-microprobe analyses of intragranitic tourmalines (tourmaline I) in wt%. 1) granite, Bence Hill, Velence (MBFSZ-5307); 2–4) pegmatite, Sukoró (2: MBFSZ-11138, 3: MBFSZ-11144, 4: MBFSZ-11149); 5) aplite, Bence Hill, Velence (MBFSZ-5304); 6) aplite, Tompos Hill, Pákozd (V3)

	1	2	3	4	5	6
SiO_2	33.91	33.86	33.12	33.91	33.34	33.80
TiO_2	0.05	0.22	0.26	0.25	0.45	0.36
B_2O_3*	9.97	9.85	9.84	9.82	9.97	9.86
Al_2O_3	28.92	27.05	26.67	26.03	29.49	27.46
Fe_2O_3**	1.71	3.00	5.35	4.47	1.97	3.15
FeO**	18.82	19.31	18.68	19.11	18.37	18.78
MgO	0.36	0.12	0.28	0.10	0.31	0.07
CaO	0.47	0.09	0.09	0.06	0.16	0.02
MnO	0.51	0.61	0.10	0.57	0.31	0.60
Na_2O	2.42	2.73	2.71	2.54	2.58	2.53
K_2O	0.00	0.00	0.00	0.00	0.00	0.00
F	0.00	0.00	0.00	0.00	0.00	0.00
H_2O***	3.44	3.40	3.39	3.39	3.44	3.40
O=F	0.00	0.00	0.00	0.00	0.00	0.00
Total	**100.58**	**100.24**	**100.49**	**100.25**	**100.38**	**100.04**
Ion numbers based on 31 (O, OH, F) anions						
Si	5.91	5.97	5.85	6.00	5.81	5.96
Al	0.09	0.03	0.15	0.00	0.19	0.04
Σ*T*	**6.00**	**6.00**	**6.00**	**6.00**	**6.00**	**6.00**
B	3.00	3.00	3.00	3.00	3.00	3.00
Σ*B*	**3.00**	**3.00**	**3.00**	**3.00**	**3.00**	**3.00**
Al	5.86	5.60	5.41	5.43	5.88	5.66
Mg	0.09	0.03	0.07	0.03	0.08	0.02
Fe^{3+}	0.05	0.37	0.52	0.54	0.04	0.32
Σ*Z*	**6.00**	**6.00**	**6.00**	**6.00**	**6.00**	**6.00**
Al	0.00	0.00	0.00	0.00	0.00	0.00
Ti	0.01	0.03	0.03	0.03	0.06	0.05
Fe^{3+}	0.17	0.03	0.19	0.05	0.22	0.10
Mg	0.00	0.00	0.00	0.00	0.00	0.00
Mn	0.08	0.09	0.01	0.09	0.05	0.09
Fe^{2+}	2.74	2.85	2.76	2.83	2.68	2.77
Σ*Y*	**3.00**	**3.00**	**3.00**	**3.00**	**3.00**	**3.00**
Ca	0.09	0.02	0.02	0.01	0.03	0.00
Na	0.82	0.93	0.93	0.87	0.87	0.86
K	0.00	0.00	0.00	0.00	0.00	0.00
[]	0.09	0.05	0.05	0.12	0.10	0.13
Σ*X*	**1.00**	**1.00**	**1.00**	**1.00**	**1.00**	**1.00**
OH	4.00	4.00	4.00	4.00	4.00	4.00
F	0.00	0.00	0.00	0.00	0.00	0.00
Σ(*V*+*W*)	**4.00**	**4.00**	**4.00**	**4.00**	**4.00**	**4.00**

* B_2O_3 calculated from the stoichiometry: B = 3 *apfu*.
** Total iron was measured as FeO. Fe_2O_3/FeO ratio calculated from equation $T + Z + Y = 15$ *apfu*.
*** H_2O calculated from the stoichiometry: OH + F = 4 *apfu*.

that the infiltrating fluid comes from a source other than the granite body is confirmed by the chemistry of the tourmaline rim, i.e., the increased Al and Mg content.

Miarolitic tourmaline (tourmaline II). Representative chemical analyses of the tourmaline II are given in Table 3. Miarolitic tourmaline shows 0.79 to 0.89 apfu Na in the X-site, so it belongs to the group of alkali tourmalines (Fig. 6). They have 5.91 to 6.06 apfu Si in the T-site, while the Z-site is fully occupied by Al. In the Y-site, the "cation deficiency" exceeds more than 0.5 apfu, which is so significant that it can only be explained by the incorporation of an element that could not be detected by the electron-microprobe, which is lithium. This is supported by the high ^{Y}Al-content (0.69–1.02 apfu), which cannot be interpreted by the substitution of ^{X}Na + ^{Y}Fe → ^{X}[] + ^{Y}Al due to the equally high ^{X}Na content. The occupancy of Li is also indicated by the occurrence of the mineral in miarolitic cavities and the greenish color of its crystals. Thus, if the total "cation deficiency" of Y is attributed to the Li content, the amount of Li varies from 0.54 to 0.98 apfu. Since the third major cation in Y besides Li and Al is Fe^{2+} (0.99–1.42 apfu), tourmaline II is an elbaite-schorl mixed crystal whose composition is around the boundary of the two mineral

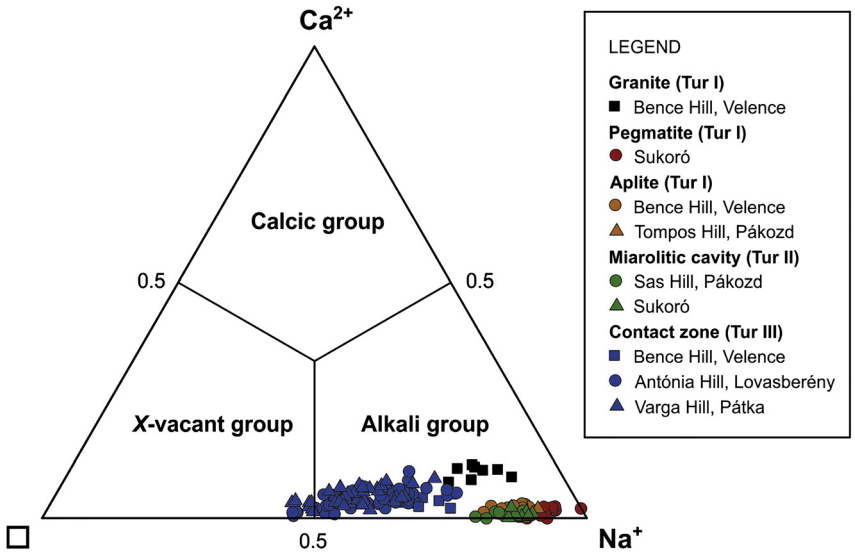

Fig. 6. Compositions of the tourmalines from the Velence Mountains plotted in a ternary diagram for the primary tourmaline groups based on the occupancy of the *X*-site

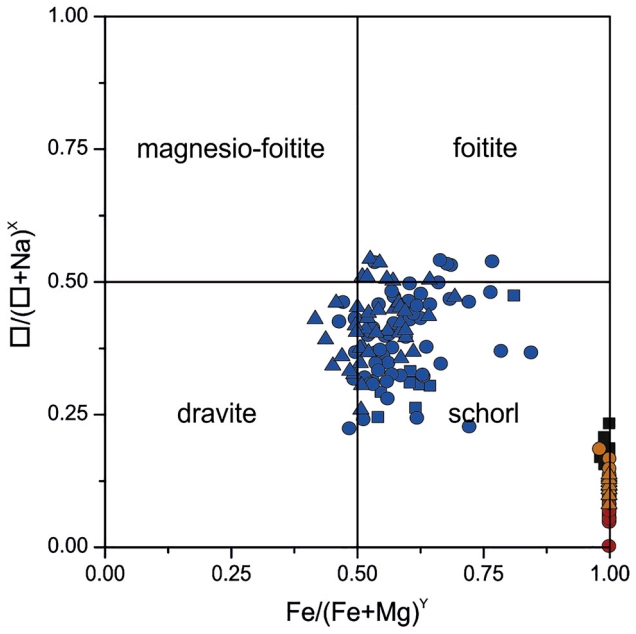

Fig. 7. Compositions of tourmalines from the Velence Mountains plotted in the $Fe/(Fe + Mg)^{Y}$ vs. $[]/([] + Na)^{X}$ diagram. For the legend see Fig. 6

species (Fig. 8). In this position, even the Mn content is significant (0.26–0.34 apfu in HOM-2009.215 and 0.06–0.12 apfu in MBFSZ-11133 samples), the Ti content is negligible (0–0.03 apfu), while the Mg content is below the detection limit. In the MBFSZ-11133 sample, zinc content was also detectable (Zn = 0.03–0.04 apfu). In the W-site, the miarolitic tourmaline shows elevated fluorine content (0.29–0.60 apfu). The positive correlation between the measured fluorine content and the calculated lithium content is well visible (Fig. 9). At some analytical points of the MBFSZ-11133 sample (Sukoró), the dominant W-anion is fluorine, so these compositions correspond to fluorelbaite species.

While sample MBFSZ-11133 (Sukoró) is chemically relatively homogeneous, sample HOM-2009.215 (Pákozd) exhibits two types of transformation zones (Fig. 5d). The type 1 zone appears as a thin infiltration inside the crystal, while the Type 2 zone occurs as a slight rim on a very small part of the crystal. The chemistry of the Type 1 zone corresponds to foitite (Table 3, Column 3), while the Type 2 zone represents schorl (Table 3, Column 4).

Metasomatic tourmaline (tourmaline III). Representative chemical analyses of the tourmaline III are given in Table 4. Metasomatic tourmaline shows fine oscillatory zonation on the BSE images. The thickness of each zone may vary from sample to sample, but is usually only a few μm. However, the crystal cores are often chemically homogeneous or mottled (Fig. 5e).

At the X-site, the amount of K is always below the detection limit, and the Ca content is consistently low (0.01–0.10 apfu). The variability is represented by the Na content and the number of vacancies, both within relatively wide ranges: 0.44–0.74 apfu Na and 0.21–0.53 apfu vacancies. Generally, the tourmaline in the contact zone is poorer in Na and richer in vacancies than the intragranitic tourmaline. Still, most tourmaline compositions show Na-dominancy in the X-site, meaning that the majority of the analytical points belong to the alkali tourmaline group and only a small proportion falls into the X-vacant group (Fig. 6).

The T-site is either completely occupied by Si or minor Al substitution exists (up to 0.23 apfu ^{T}Al). The Z-site is almost always occupied by Al alone. The Y-site shows the usual mixed cation occupancy. Due to the high number of vacancies in X, the ^{Y}Al content can be significant (up to 0.91 apfu) via the substitution $^{X}Na + {}^{Y}(Fe, Mg) \rightarrow {}^{X}[] + {}^{Y}Al$. The

Table 3. Representative electron-microprobe analyses of miarolitic tourmalines (tourmaline II) in wt%. 1) Sukoró (MBFSZ-11133); 2–4) Sas Hill, Pákozd (HOM-2009.215; 2: elbaite-schorl core, 3: Type 1 zone, 4: Type 2 zone)

	1	2	3	4
SiO_2	36.62	35.54	35.15	35.17
TiO_2	0.03	0.22	0.06	0.16
B_2O_3*	10.60	10.37	10.21	10.19
Al_2O_3	36.05	34.21	33.55	32.02
FeO**	7.60	9.75	15.28	16.38
MgO	0.00	0.00	0.01	0.00
CaO	0.02	0.00	0.01	0.07
MnO	0.61	2.38	0.39	0.27
ZnO	0.28			
Li_2O***	1.32	0.81	0.07	0.24
Na_2O	2.76	2.51	1.03	2.00
K_2O	0.00	0.00	0.00	0.00
F	1.08	0.63	0.00	0.00
H_2O****	3.15	3.28	3.52	3.52
O=F	0.46	0.27	0.00	0.00
Total	**99.67**	**99.43**	**99.29**	**100.01**
Ion numbers based on 31 (O, OH, F) anions				
Si	6.00	5.96	5.98	6.00
Al	0.00	0.04	0.02	0.00
Σ*T*	**6.00**	**6.00**	**6.00**	**6.00**
B	3.00	3.00	3.00	3.00
Σ*B*	**3.00**	**3.00**	**3.00**	**3.00**
Al	6.00	6.00	6.00	6.00
Σ*Z*	**6.00**	**6.00**	**6.00**	**6.00**
Al	0.96	0.72	0.71	0.44
Ti	0.00	0.03	0.01	0.02
Mg	0.00	0.00	0.00	0.00
Mn	0.08	0.34	0.06	0.04
Fe^{2+}	1.04	1.37	2.17	2.34
Zn	0.03			
Li	0.87	0.55	0.05	0.17
Σ*Y*	**3.00**	**3.00**	**3.00**	**3.00**
Ca	0.00	0.00	0.00	0.01
Na	0.88	0.82	0.34	0.66
K	0.00	0.00	0.00	0.00
[]	0.12	0.18	0.66	0.33
Σ*X*	**1.00**	**1.00**	**1.00**	**1.00**
OH	3.44	3.67	4.00	4.00
F	0.56	0.33	0.00	0.00
Σ(*V*+*W*)	**4.00**	**4.00**	**4.00**	**4.00**

* B_2O_3 calculated from the stoichiometry: B = 3 *apfu*.
** Total iron was measured as FeO.
*** Li_2O calculated from the stoichiometry: $\Sigma Y = 3$ *apfu*.
**** H_2O calculated from the stoichiometry: OH + F = 4 *apfu*.

Y-position is dominated by Fe^{2+} and Mg. While the amount of Mg in the intragranitic and miarolitic tourmalines is negligible, the tourmaline of the contact zone exhibits a high amount of Mg (0.32–1.38 apfu), so much that it is the dominant Y-cation at some analyzed points. The amount of Fe^{2+} ranges from 0.89 to 2.00 apfu. The amount of Ti and Mn is not significant, with maxima 0.11 and 0.04 apfu, respectively. In the tourmaline dominated by vacancies in X, Fe^{2+} is always the most abundant cation in Y, so the tourmaline of the contact rocks represents schorl, dravite, and foitite in descending order of frequency, while the magnesio-foititic composition is absent (Fig. 7).

The zonation observed in the back-scattered electron images is basically caused by different Fe and Mg contents at the Y-site. The lighter zones are richer in iron, while the darker ones are richer in magnesium. However, if the Fe content of the tourmaline is plotted against Mg content (Fig. 10a), the correlation coefficient is rather low; therefore, the role of homovalent $Fe^{2+} \leftrightarrow Mg$ substitution is not significant. Instead, the coupled heterovalent substitutions among each zone could be more important. The cation-deficient foitite–magnesio–foitite series of $[][(Fe, Mg)_2Al]Al_6Si_6O_{18}(BO_3)_3(OH)_4$ is achieved from the schorl-dravite series of $Na(Fe, Mg)_3Al_6Si_6O_{18}(BO_3)_3(OH)_4$ by the coupled

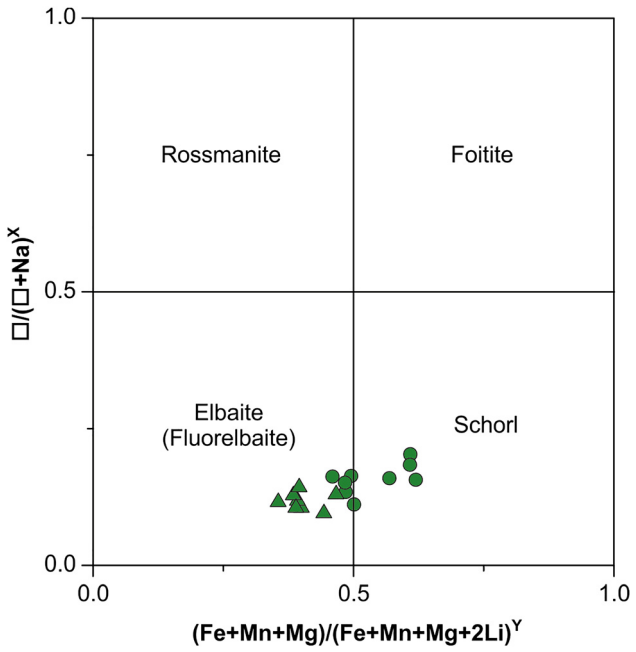

Fig. 8. Compositions of Li-bearing tourmalines of the miarolitic cavities (tourmaline II) plotted in the (Fe + Mn + Mg)/(Fe + Mn + Mg + 2Li)^{Y} vs. []/([] + Na)^{X} diagram. For the legend see Fig. 6

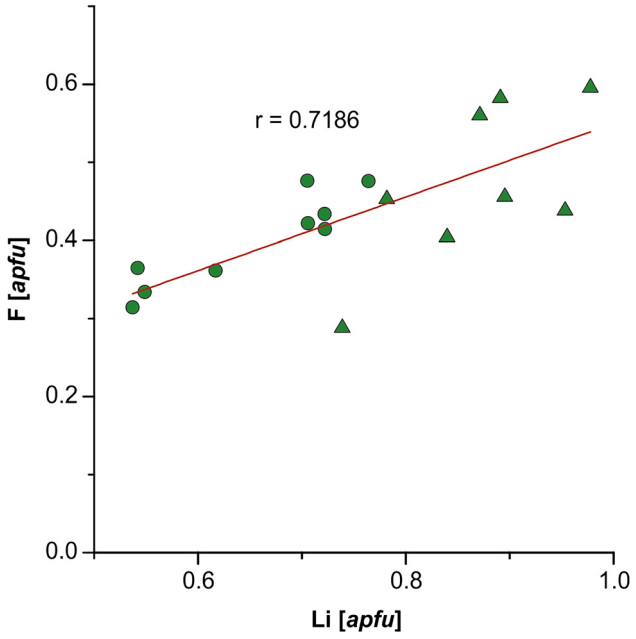

Fig. 9. Representation of the Li content of the miarolitic tourmalines (tourmaline II) as a function of F content (r = correlation coefficient). Spheres = sample HOM-2009.215 (Sas Hill, Pákozd), triangles = sample MBFSZ-11133 (Sukoró)

substitution of ^{X}Na + ^{Y}(Fe, Mg) = ^{X}[] + ^{Y}Al. This substitution mechanism also operates in tourmaline III with high correlation coefficient (Fig. 10b). As the amount of ^{X}Ca can be well measured at some analyzed points (up to 0.10 apfu), therefore the substitution of ^{X}Ca + ^{Y}(Fe, Mg) → ^{X}Na + ^{Y}Al should also be considered. Its correlation coefficient, and thus its effect on the composition of tourmaline III, is slightly smaller (Fig. 10c) but still very high. This may be due to the low Ca content compared to vacancies. Fig. 10d shows in tourmaline III, the so-called alkali-deficient substitution, ^{X}Na + ^{Y}(Fe, Mg) = ^{X}[] + ^{Y}Al, prevails over the so-called proton-deficient substitution ^{Y}(Fe, Mg) + ^{W}(OH) = ^{Y}Al + ^{W}O. This is partly due to the formula calculation method: if the formula calculation had been performed for 15 (T + Z + Y) cations, the cation deficiency in Y-site would have disappeared by replacing (OH) at the W position with some O^{2-}, which would have slightly shifted the substitution trend towards the proton-deficient type.

DISCUSSION

Jantsky (1957) considered tourmalines of the Velence Mountains to be uniformly of pneumatolytic origin, whether occurring in the granite and its vein rocks or in the contact slate and their quartz-tourmaline veinlets. As he wrote: "it is not justified to infer genetic differences from the color, size or pleochroism of tourmaline. The structural differences can be traced back to different physicochemical conditions and different environments of crystallization". Based on the present studies, this simple genetic picture needs to be slightly tinged. Intragranitic tourmaline is considered to be crystallized in a closed fluid-melt system based on the lack of chemical zonation and its predominantly disseminated arrangement in the rocks, according to Jolliff et al. (1986) and London and Manning (1995). Only tourmaline present in the miarolitic cavities or associated with contact slate is regarded as pneumatolytic or, as it is known today, high-temperature hydrothermal and hydrothermal-metasomatic phase. In this chapter, we first look for the reason for the very scarce occurrence of tourmaline in the granite and its derivative rocks, and then outline the most likely scenario of tourmaline formation that our data currently provides.

Tourmaline appears only rarely and always in negligible quantities in the granite and its vein rocks in the Velence Mountains. More abundant formation of tourmaline is associated with the contact metamorphic aureole surrounding the granite. What could be the reason that the formation of tourmaline in granite was so insignificant? Let us see what the main conditions for the formation of tourmaline in granitic systems are! Here the focus is primarily on chemical conditions and not with intensive variables such as temperature or pressure due to the high stability field of tourmaline (the upper stability limits, depending on the composition, are 725–950 °C and 50–70 kbar; van Hinsberg et al., 2011).

The first and most important condition for the formation of tourmaline is the presence of a sufficient amount of boron in the system. According to Buda (1993), the Velence Granite was crystallized from water-saturated, eutectic melt at 680 °C. Under these conditions, according to London (1999), the content of B_2O_3 required to saturate tourmaline in granitic melts is about 2 wt%. The following literature

Table 4. Representative electron-microprobe analyses of metasomatic tourmalines (tourmaline III) in wt%. 1–2) Bence Hill, Velence (MBFSZ-5301); 3–10) Antónia Hill, Lovasberény (3–4: MBFSZ-5297, 5–6: HOM-18142, 7–8: HOM-17701, 9–10: HOM-25922); 11–16) Varga Hill, Pátka (11–12: HOM-23596, 13–14: HOM-26284, 15–16: V1)

	1	2	3	4	5	6	7	8
SiO_2	35.93	36.31	34.72	35.25	34.78	35.68	36.18	35.64
TiO_2	0.56	0.68	0.75	0.54	0.62	0.62	0.36	0.42
B_2O_3*	10.44	10.44	10.26	10.50	10.35	10.44	10.50	10.53
Al_2O_3	31.75	30.73	30.45	32.93	33.74	32.91	34.41	34.08
Fe_2O_3**			1.05	1.00				
FeO**	12.02	12.30	14.14	10.24	12.80	9.54	10.34	8.29
MgO	4.06	4.30	3.21	4.58	1.96	4.34	2.75	4.76
CaO	0.18	0.21	0.29	0.17	0.22	0.23	0.08	0.30
MnO	0.00	0.10	0.00	0.00	0.13	0.24	0.00	0.00
Na_2O	2.08	2.20	2.23	1.82	1.86	1.90	1.43	2.02
K_2O	0.00	0.00	0.00	0.00	0.00	0.00	0.00	0.00
F	0.00	0.00	0.00	0.00	0.00	0.00	0.00	0.00
H_2O***	3.60	3.60	3.54	3.62	3.57	3.60	3.62	3.63
O=F	0.00	0.00	0.00	0.00	0.00	0.00	0.00	0.00
Total	**100.62**	**100.87**	**100.64**	**100.65**	**100.03**	**99.51**	**99.67**	**99.68**
Ion numbers based on 31 (O, OH, F) anions								
Si	5.98	6.05	5.88	5.84	5.84	5.94	5.99	5.88
Al	0.02	0.00	0.12	0.16	0.16	0.06	0.01	0.12
Σ*T*	**6.00**	**6.05**	**6.00**	**6.00**	**6.00**	**6.00**	**6.00**	**6.00**
B	3.00	3.00	3.00	3.00	3.00	3.00	3.00	3.00
Σ*B*	**3.00**	**3.00**	**3.00**	**3.00**	**3.00**	**3.00**	**3.00**	**3.00**
Al	6.00	6.00	5.96	6.00	6.00	6.00	6.00	6.00
Mg	0.00	0.00	0.04	0.00	0.00	0.00	0.00	0.00
Σ*Z*	**6.00**	**6.00**	**6.00**	**6.00**	**6.00**	**6.00**	**6.00**	**6.00**
Al	0.21	0.03	0.00	0.26	0.52	0.39	0.71	0.51
Ti	0.07	0.09	0.10	0.07	0.08	0.08	0.04	0.05
Fe^{3+}			0.13	0.12				
Mg	1.01	1.07	0.77	1.13	0.49	1.08	0.68	1.17
Mn	0.00	0.01	0.00	0.00	0.02	0.03	0.00	0.00
Fe^{2+}	1.67	1.71	2.00	1.42	1.80	1.33	1.43	1.14
Σ*Y*	**2.96**	**2.91**	**3.00**	**3.00**	**2.90**	**2.91**	**2.86**	**2.88**
Ca	0.03	0.04	0.05	0.03	0.04	0.04	0.01	0.05
Na	0.67	0.71	0.73	0.58	0.61	0.61	0.46	0.65
K	0.00	0.00	0.00	0.00	0.00	0.00	0.00	0.00
[]	0.30	0.25	0.22	0.39	0.35	0.35	0.52	0.30
Σ*X*	**1.00**	**1.00**	**1.00**	**1.00**	**1.00**	**1.00**	**1.00**	**1.00**
OH	4.00	4.00	4.00	4.00	4.00	4.00	4.00	4.00
F	0.00	0.00	0.00	0.00	0.00	0.00	0.00	0.00
Σ(*V*+*W*)	**4.00**	**4.00**	**4.00**	**4.00**	**4.00**	**4.00**	**4.00**	**4.00**

(continued)

data are available on the boron content of the Velence Granite: 10–25 ppm (Nagy, 1967b), 14–49 ppm (Pantó, 1977), 14 ppm (Horváth et al., 1989) and 8–35 ppm (Uher and Broska, 1994). It can be seen that the Velence Granite contains orders of magnitude less boron than what would have been sufficient for the formation of tourmaline. The question may be to what extent the boron content of the granite reflects that of the original granitic melt? The answer is: to no extent. According to London et al. (1996), whole-rock analyses of granites offer no quantitative appraisal of the boron content of their magmas if buffering reactions that conserve boron in crystalline phases did not operate down to solidus conditions. The magmas preserve their boron content as much as they retain their water; in other words, boron is preferably secreted into the volatile phase in melt-volatile systems (Benard et al., 1985). Thus, there is no reason to suppose that the Velence Granite, containing boron only as a trace element, could not contain much more significant quantities of boron even in the molten phase. This is supported by the presence of tourmaline in the contact slate surrounding the granite, in some places even in considerable quantities.

Let us suppose that the amount of boron needed to form tourmaline in the granitic melt was available and see how other geochemical factors have promoted or inhibited the precipitation of tourmaline. After the boron content, the aluminosity of the melt (rock) is an important parameter. It is emphasized that this parameter is not only about the aluminum content, but about the ratio of aluminum to calcium plus sodium and potassium. The measure of

Table 4. **Continued**

	9	10	11	12	13	14	15	16
SiO_2	35.47	35.80	35.31	35.34	35.51	35.47	35.07	35.74
TiO_2	0.81	0.21	0.09	0.37	0.52	0.90	0.84	0.38
B_2O_3*	10.33	10.67	10.44	10.47	10.60	10.54	10.39	10.50
Al_2O_3	31.61	35.83	33.45	34.00	34.72	33.93	32.44	33.31
FeO**	11.51	9.04	10.90	8.29	9.79	7.93	10.90	8.64
MgO	3.79	3.84	4.13	4.77	3.87	5.01	4.30	5.13
CaO	0.32	0.29	0.10	0.26	0.30	0.41	0.44	0.25
MnO	0.07	0.07	0.10	0.02	0.32	0.02	0.00	0.05
Na_2O	1.95	1.56	1.84	2.00	1.72	1.86	1.83	1.99
K_2O	0.00	0.00	0.00	0.00	0.00	0.00	0.00	0.00
F	0.00	0.00	0.00	0.00	0.00	0.00	0.00	0.00
H_2O***	3.56	3.68	3.60	3.61	3.66	3.64	3.59	3.62
O=F	0.00	0.00	0.00	0.00	0.00	0.00	0.00	0.00
Total	**99.42**	**100.99**	**99.96**	**99.14**	**101.00**	**99.71**	**99.80**	**99.62**
Ion numbers based on 31 (O, OH, F) anions								
Si	5.97	5.83	5.88	5.87	5.82	5.85	5.86	5.91
Al	0.03	0.17	0.12	0.13	0.18	0.15	0.14	0.09
Σ*T*	**6.00**	**6.00**	**6.00**	**6.00**	**6.00**	**6.00**	**6.00**	**6.00**
B	3.00	3.00	3.00	3.00	3.00	3.00	3.00	3.00
Σ*B*	**3.00**	**3.00**	**3.00**	**3.00**	**3.00**	**3.00**	**3.00**	**3.00**
Al	6.00	6.00	6.00	6.00	6.00	6.00	6.00	6.00
Σ*Z*	**6.00**	**6.00**	**6.00**	**6.00**	**6.00**	**6.00**	**6.00**	**6.00**
Al	0.24	0.71	0.44	0.52	0.53	0.44	0.26	0.41
Ti	0.10	0.03	0.01	0.05	0.06	0.11	0.11	0.05
Mg	0.95	0.93	1.03	1.18	0.95	1.23	1.07	1.27
Mn	0.01	0.01	0.01	0.00	0.04	0.00	0.00	0.01
Fe^{2+}	1.62	1.23	1.52	1.15	1.34	1.09	1.52	1.20
Σ*Y*	**2.92**	**2.91**	**3.01**	**2.90**	**2.93**	**2.88**	**2.96**	**2.93**
Ca	0.06	0.05	0.02	0.05	0.05	0.07	0.08	0.04
Na	0.64	0.49	0.59	0.64	0.55	0.59	0.59	0.64
K	0.00	0.00	0.00	0.00	0.00	0.00	0.00	0.00
[]	0.31	0.46	0.39	0.31	0.40	0.33	0.33	0.32
Σ*X*	**1.00**	**1.00**	**1.00**	**1.00**	**1.00**	**1.00**	**1.00**	**1.00**
OH	4.00	4.00	4.00	4.00	4.00	4.00	4.00	4.00
F	0.00	0.00	0.00	0.00	0.00	0.00	0.00	0.00
Σ(*V*+*W*)	**4.00**	**4.00**	**4.00**	**4.00**	**4.00**	**4.00**	**4.00**	**4.00**

* B_2O_3 calculated from the stoichiometry: B = 3 *apfu*.
** Total iron was measured as FeO. Fe_2O_3/FeO ratio calculated from equation $T + Z + Y = 15$ *apfu*.
*** H_2O calculated from the stoichiometry: OH + F = 4 *apfu*.

aluminosity in the melt is the alumina saturation index (ASI), which is expressed as the $Al_2O_3/(Na_2O + K_2O + CaO)$ ratio in a percentage of molecular weight (Shand, 1943). Accordingly, a distinction is made between peralkaline, metaluminous and peraluminous granites, and their discrimination diagram is shown in Fig. 2, representing the composition of the Velence Granite and its vein rocks. The figure clearly shows the weak peraluminous or even metaluminous character of the Velence rocks. The metaluminous-to-peraluminous boundary is at ASI = 1, above which free aluminum remained in the system unused by the crystallization of feldspar. Since tourmaline is a highly peraluminous mineral, its formation requires an ASI of more than 1.2–1.3 (London et al., 1996; Wolf and London, 1997). According to Fig. 2, most sites in the Velence Granite simply did not have enough aluminum for the formation of tourmaline. There is no better proof for this than the crystal-chemistry of the analyzed intragranitic tourmaline, where the Al content was below the ideal 6 apfu at almost every analytical point. Since the Mg content of the melt was also very low (Mg being one of the major substitutes for Al at the Z-site of tourmaline), tourmaline formation was only possible where sufficient Fe^{3+} was available to replace Al. Therefore, this could be one of the main reasons for the very sparse appearance, richness of iron and deficiency of aluminum in the Velence Mountain intragranitic tourmaline.

In granitic melts, the formation of tourmaline may be inhibited by the small amounts of the available femic components (Fe, Mg) as well as other mafic minerals that incorporate these elements into their lattice at the expense of tourmaline. In this respect, biotite is the most notable "opponent" of tourmaline. On several occasions (e.g., Čech, 1963; Benard et al., 1985; Pesquera et al., 2013) it has been observed that granites rich in biotite do not contain or have little tourmaline, and vice versa. In the Velence Mountains, Jantsky (1957) mentioned that the tourmaline-bearing parts

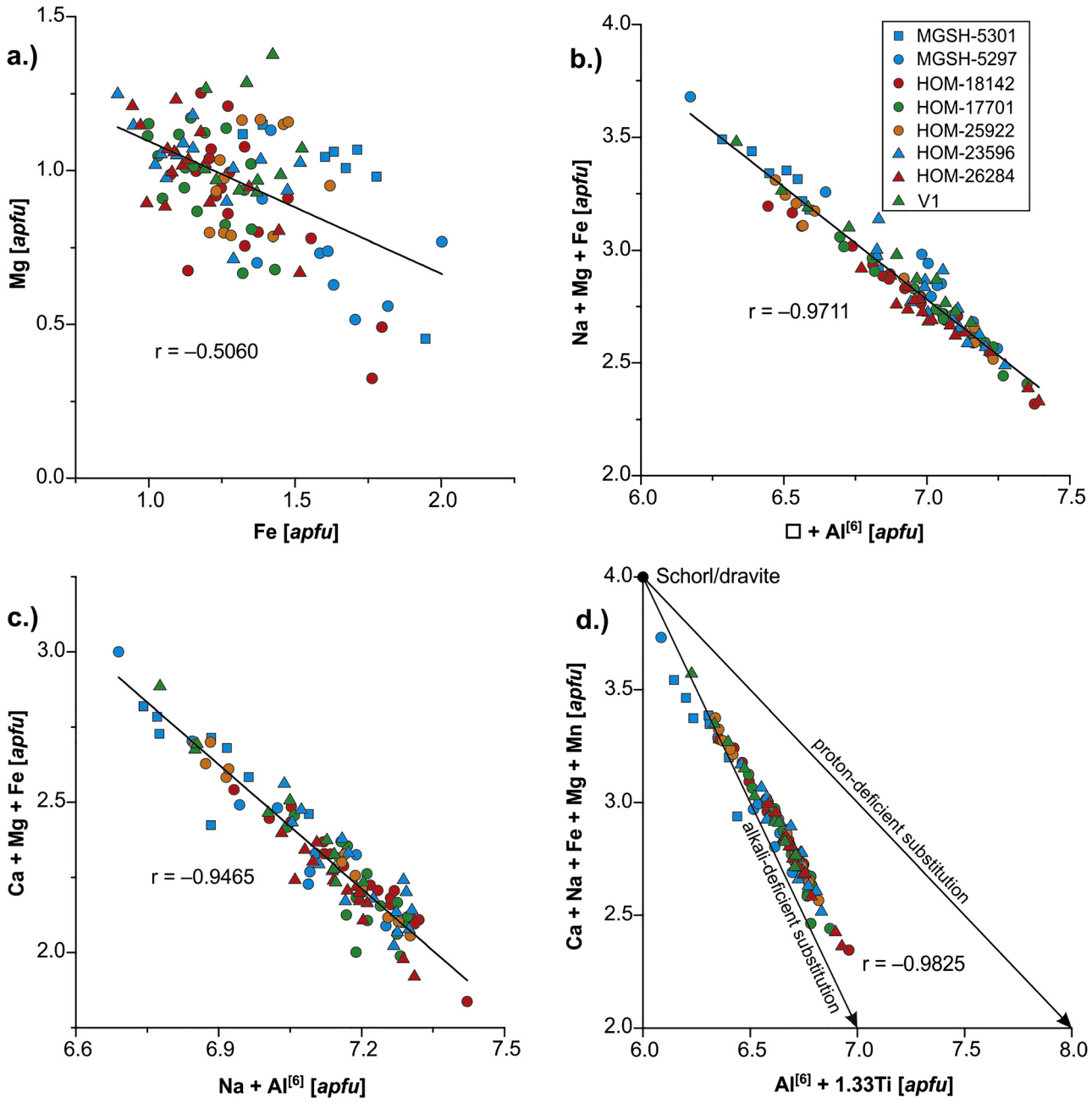

Fig. 10. Substitution mechanisms in tourmaline III. a.) Representation of the Fe content as a function of Mg; b.) Plotting of [] + $Al^{[6]}$ vs. Na + Mg + Fe; c.) Plotting of Na + $Al^{[6]}$ vs. Ca + Mg + Fe; d.) Plotting of $Al^{[6]}$ + 1.33Ti vs. Ca + Na + Fe + Mg + Mn (r = correlation coefficient)

of the aplitic granite vein from the quarry of Székesfehérvár are biotite-free or biotite-poor. The cause of the incompatibility between biotite and tourmaline has not yet been resolved. Some authors consider the water content of granitic melt to be the main factor (Guillot and Le Fort, 1995; Scaillet et al., 1995), i.e., high water content promotes biotite formation. Other researchers suggest that the Ti concentration of the melt controls the relative stability of biotite and tourmaline, such that Ti can stabilize biotite at the expense of tourmaline (Nabelek et al. 1992). Whatever is the case, it seems clear that biotite formation may have been one of the barriers to the crystallization of intragranitic tourmaline in the Velence Granite.

For the formation of tourmaline, some scientists still attach importance to the phosphorus and fluorine content of the granitic melt. Phosphorus has a strong tendency to form complexes with excess aluminum in the granitic melt, thereby reducing the stability of tourmaline by reducing the activity of aluminum in the melt (Wolf and London, 1997). As the content of phosphorus is negligible (up to 0.13 wt% P_2O_5; Uher and Broska, 1994) and phosphate minerals are minor constituents in the Velence Granite (Szakáll et al.,

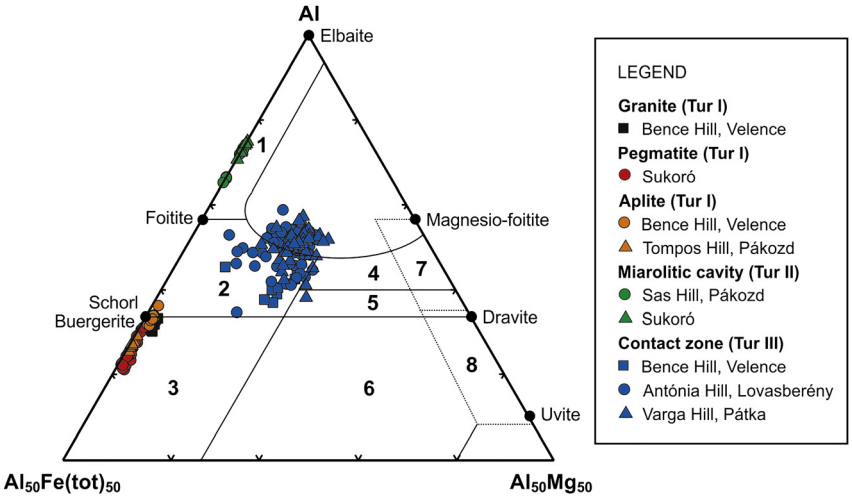

Fig. 11. Chemical composition of tourmalines of the Velence Mountains plotted in the Al–Fe(tot)-Mg ternary diagram of Henry & Guidotti (1985). Compositional fields: 1 = Li-rich granitoid pegmatites and aplites; 2 = Li-poor granitoids and their associated pegmatites and aplites; 3 = Fe^{3+}-rich quartz-tourmaline rocks (hydrothermally altered granites); 4 = metapelites and metapsammites coexisting with an Al-saturating phase; 5 = metapelites and metapsammites not coexisting with an Al-saturating phase; 6 = Fe^{3+}-rich quartz-tourmaline rocks, Ca-silicate rocks, and metapelites; 7 = low-Ca metaultramafics and Cr–V-rich metasediments; 8 = metacarbonates and metapyroxenites

2007; Ondrejka et al., 2018), the effect of phosphorus on the formation of tourmaline can be neglected. However, the role of fluorine is worth examining.

Wolf and London (1997) argue that increasing fluorine content in granitic melt also reduces the stability field of tourmaline due to complexation with Al in the melt: the more fluorine the melt contains, the higher B content and/or higher ASI required to saturate tourmaline. In relation to the Velence Granite, fluorine is basically bound in fluorite. In this respect, Jantsky (1957) distinguished between fluorite-bearing granite (e.g., at Bence Hill, Velence) and hydrothermal fluorite veins (e.g., Kőrakás Hill and Szűzvár Mill at Pátka; Zsellér field at Pákozd) in the western part of the mountain, where the latter were mined. Jantsky (1957) and many later authors (e.g., Molnár, 2004) have linked fluorite formation to granite magmatism, while others have linked it to Triassic (Benkó et al., 2014) or to Cretaceous (Horváth et al., 1989) magmatic processes. If fluorite formation is not related to granitic magmatism, the presence of large amounts of fluorite in veins does not reveal anything about the fluorine content of the former granitic melt; however, fluorite, which appears as an accessory constituent in the rock, may still indicate a slightly elevated F content in the granite. Among the common constituents of the Velence Granite, only biotite can accommodate fluorine into its lattice. Unfortunately, Buda el al. (2004a) in their article about the biotite of granites of Central Europe do not provide data on fluorine content. Uher and Broska (1996) report two biotite analyses from the Velence Granite with an F content of 0.47 and 0.56 wt%, corresponding to 0.12 and 0.15 apfu in the formula for 12 anions, respectively. According to Uher and Broska (1996) these values are higher than normal in common granite rocks, indicating high activity of fluorine. However, it should be noted that the intragranitic tourmaline of Velence (which is also able to bind fluoride) has a fluorine content below the detection limit.

Thus, even if the melt of the Velence Granite contained sufficient boron to saturate tourmaline, its relatively low Al content, the low proportion of femic components (Fe, Mg) and their incorporation into biotite lattice were effective against the formation of tourmaline.

Next, let us review the most likely scenario for the formation of tourmaline of the Velence Granite. After the major Devonian-Carboniferous collisional, and Carboniferous transpressional stages, transtensional to extensional relaxation regimes were achieved from 300 ± 20 Ma (Neugebauer, 1988). According to Uher and Broska (1996), if the mean MOHO level of a thinning, highly eroded continental crust within a large strike-slip fault zone of post-orogenic region, is assumed at around 25–30 km, lower crustal levels around 20 km could contribute sites of partial anatexis of older acidic rocks, including the protolith of the Velence Granite. According to the above authors, the protolith itself may have been some granulite facies metamorphite and the rare mafic enclaves described by Buda (1993) could be a marker of unmixing or anatexis from more basic lower crustal to upper mantle protolith. This is somewhat contradicted by the presumably elevated boron content of the granitic melt. If this boron originated from the protolith and did not assimilate from the wall rock during the ascent of the granitic magma, the granulite protolith must have included a boron-containing mineral, one that could remain stable under the granulite facies conditions. It was most likely, due to its frequency, the tourmaline itself. If a partial melting of a tourmaline-containing meta-sediment occurs at low temperatures, most of the tourmaline is likely to remain in the protolith, since the mineral is essentially insoluble in low-temperature granitic melts. The partial melting temperature must have been higher than 750 °C, since at least this

temperature is required for the tourmaline to react and release the stored amount of boron (Benard et al., 1985).

Melt ascent from the zone of partial anatexis to the zone of final emplacement and solidification was favored by the transtensional or extensional tectonic environment along huge and deep strike-slip fault systems (Uher and Broska, 1996; Benkó et al., 2014). Since boron reduces the viscosity of the melt, the presumed boron content of granitic magma may have promoted the melt reaching a shallower depth. Rising to a hypabyssal level (6–8 km), the magma had shifted into slate that had previously undergone anchizonal regional metamorphism. Typological analysis of zircon of the granite indicates a relatively high crystallization temperature of 800 °C (Uher and Broska 1994), which can be considered as the liquidus temperature of the Velence Granite (Uher and Broska 1996). First, biotite crystallized at 680 °C (Buda et al., 2004a), followed by potassium feldspar (orthoclase) and quartz crystallization at 630–650 °C (Buda, 1969, 1981); finally, plagioclase precipitation occurred at 520 °C (Buda, 1969). At this stage of the granite crystallization, the boron content of the magma could not yet have been high enough to saturate the melt for tourmaline.

It is conceivable that the residual granitic melt never reached the boron content (ca. 2 wt% B_2O_3) that would have been sufficient for tourmaline formation. It is likely that the precipitation of tourmaline could only begin with the appearance of an exsolving aqueous fluid in a closed melt-fluid system where an aqueous fluid interface was present between the melt and the crystallizing tourmaline. Where disseminated tourmaline crystals appear in the rock, i.e., with one exception for all intragranitic samples, the tourmaline precipitation occurred at a temperature higher than the solidus of the granite.

Nor can the possibility be completely ruled out that some of the intragranitic tourmaline crystallized directly from the melt in a system without an exsolved fluid phase. This may be indicated by the disseminated arrangement of tourmaline crystals in the rocks and the lack of chemical zonation in the tourmaline crystals (see London and Manning, 1995). However, the existence of a melt-aqueous fluid system is made possible by several factors:

1. In granitic systems, boron is preferentially separated into the fluid phase. Only highly fractionated residual melts of inherently high B-content magmas are able to achieve the 2 wt% B_2O_3 content required to saturate tourmaline (London and Manning, 1995). However, it is much more likely that the exsolved fluid rising through the melt may have caused differentiation by depleting lower portions of the melt for the elements that favor the fluid (e.g., boron), thus enriching the melt in the upper parts for these same elements (Jolliff et al., 1986).
2. In the Velence Granite, pegmatites, and aplites, the $Fe_{tot}/(Fe_{tot} + Mg)$ ratio (calculated from atomic percentages) mostly ranges from 0.73 to 0.80 (see analytical data in Fig. 2), which essentially reflects similar values measured in biotite (see data from Uher and Broska, 1996 and Buda et al., 2004a). In contrast, the $Fe_{tot}/(Fe_{tot} + Mg)$ ratio in the intragranitic tourmaline is significantly higher, ranging from 0.95 to 0.99. Since iron is favorably partitioned into aqueous fluid coexisting with the silicate melt, while magnesium is strongly retained in the melt (Jolliff et al., 1986), the enrichment of tourmaline in iron over granite/biotite also suggests the presence of fluid.
3. In the Bence Hill aplite (sample MBFSZ-5304), tourmaline forms a thick veinlet, which clearly indicates precipitation from solution, and its chemical composition is essentially the same as that of other intragranitic tourmalines.

The genetic interpretation of intragranitic tourmaline is somewhat complicated by their pronounced (although calculated) Fe^{3+} content, which can reach up to 0.76 apfu. Such Al-undersaturated and Fe^{3+}-containing tourmaline from NYF-type pegmatites of the Třebíč pluton (Bohemia) have already been mentioned as the primary magmatic phase (Novák et al., 2011), although they were also rich in Ca and Ti. The point is that the low Al and perceptible Fe^{3+} content of intragranitic tourmaline of the Velence Granite do not preclude their primary magmatic origin. However, it should be noted that a significant proportion of biotite is also oxidized, with $Fe^{3+}/(Fe^{3+} + Fe^{2+}) = 0.27$ on average, which reveals a secondary origin (Buda et al., 2004a), which can be attributed to the auto-metamorphic/auto-metasomatic/autohydration effect of volatiles separated from the melt in the late stages of magmatic mineralization. Thus, it cannot be ruled out that auto-metasomatic processes also played a role in the oxidation of the tourmaline in the Velence Mts.

The tourmaline crystals of the Sukoró pegmatite later disintegrated; the cracks among the fragments were filled with an association of quartz and potassium feldspar, and the latter subsequently kaolinized. A thin foititic reaction rim (up to 3 μm in thickness) was formed at the edge of some tourmaline fragments by fluid infiltration, probably at the same time as the formation of quartz-potassium feldspar fillings, and/or with the kaolinization of the K-feldspar. The infiltrating fluid must come from a different/outside source than the granite, because of its much higher Mg-content. This fluid may have been generated by Paleogene volcanism, or may also have been derived from the older Triassic magmatic activity.

Since the conditions for the formation of tourmaline from magma were generally not favorable, the majority of the boron in the granitic melt passed into the separated fluid phase. These fluids were also slightly enriched in fluorine and lithium in addition to boron, although most of the fluorine could have been precipitated as fluorite (if fluorite formation is related to granitic magmatism) or, to a lesser extent, incorporated into the structure of biotite. In some of the pegmatites, miarolitic cavities produced greenish-black, greyish-green tourmaline from these solutions, which, unlike intragranitic tourmaline, contain high levels of Al and significant amounts of Li and F. Thus, this miarolitic tourmaline belongs to the schorl-elbaite series. The positive correlation between Li and F can be clearly observed. With

the higher Li content, more fluorine can be measured in the tourmaline. Thus, at some analytical points, a fluor-elbaite composition also appeared. Since these tourmalines do not show any chemical zonation, they were formed in a closed system, meaning that the constituents from the country rock were not involved in their composition. However, in the Sas Hill sample, after the formation of tourmaline II, the cavity could open, and the schorl–elbaite mixed crystals were transformed to schorl and foitite at the edges or cracks as a result of the fluid infiltration from outside.

The majority of the boron-enriched hydrothermal solutions, which separated from the granite, metasomatized the adjacent slate mantle, creating tourmaline-bearing hornfels and quartz-tourmaline veins. The formation of tourmaline III had already taken place in an open system, as evidenced by the well-visible, sometimes oscillatory zoning of the tourmaline crystals, which has no systematic chemical trend from the core to the edge of the crystals. Chemically, this tourmaline is also very different from the intragranitic samples, reflecting, to some extent, the composition of host slate. The main differences are elevated Al and Mg content, significantly increased vacancies at the X-site, and decreasing Na and Fe content. It can be stated that there is no overlap between the chemical composition of magmatic (intragranitic) and hydrothermal (contact rocks, quartz-tourmaline veins) tourmalines (Fig. 11).

Lower Permian post-orogenic A-type granites related to the Velence Granite also occur in the Western Carpathians, Slovakia: Turčok (Uher and Gregor, 1992), Hrončok (Petrík et al., 1995), the Kohút Zone (Hraško et al. 1997), and as pebbles or boulders in Cretaceous–Paleogene conglomerates (i.e., Upohlav granites; Uher et al., 1994). So far tourmaline was mentioned only from the granites of Turčok and the Kohút Zone without more detailed mineralogical studies.

CONCLUSIONS

Granitic magma is derived from the anatectic melting of a crust unit dominated by granulites (metapelites?) containing feldspar, ferromagnesian minerals and possibly tourmaline.

As the magma rose and cooled, the exsolved aqueous fluid caused differentiation by depleting lower portions of melt of the elements that favor the fluid phase (e.g., boron), thus enriching melt in upper parts of the system in them. In some places, after reaching a sufficient concentration of boron, the reaction of ferromagnesium minerals produced extremely limited amounts of tourmaline in closed melt-aqueous fluid systems. Due to the limited formation of tourmaline, much of the boron remained in the residual fluid phase, which migrated to the country rock and was involved in metasomatic processes.

Tourmaline from a variety of environments exhibits considerable variation in composition, which is controlled by the nature of the host rock and the formation processes. However, in similar geologic situations, the composition of tourmaline could be rather uniform, even among relatively distant localities (e.g., the aplites of Bence and Tompos Hills, or the contact slates of Antónia and Varga Hills). In this sense the composition of tourmaline represents important details of the environment in which they were formed.

The pitch-black tourmaline in the granite, pegmatites and aplites represents the schorl species. It is characterized by low total Al content, which is usually below 6 apfu. Another important feature is its elevated iron content, where a significant amount of iron is present as Fe^{3+}.

In a closed melt-aqueous fluid system that does not undergo rapid change, the pressure, temperature, and composition gradually change, so the crystalline magmatic phases (such as tourmaline) show little chemical diversity. The disseminated tourmaline of the granite, pegmatites and aplites corresponds to these properties and is therefore considered to be the primary magmatic phase. However, significant Fe^{3+} content may indicate auto-metasomatic transformation.

The fluid phase separated from the granite but still circulating in the rock is enriched in various incompatible elements (like boron, fluorine, lithium, manganese, etc.). As no material was added to the fluids in the miarolitic cavities from outside sources, the precipitated tourmalines are fluorine-containing schorl-elbaite mixed crystals without significant chemical variation, i.e., mineral formation still occurred in a chemically closed system. However, after the cavities had opened, the tourmaline of the Sas Hill sample was partly transformed into schorl and foitite.

Since the requirements for tourmaline formation did not exist (e.g., due to the lack of femic components), the B content of the granitic melt increased without further control until the system was opened to contact-external fluids or rocks that provided the reactive components (Fe and Mg) for further tourmaline formation. The amount of boron that was not conserved in the crystalline phases of the closed magmatic system was deposited as tourmaline when the magmatic system opened to the surrounding rocks.

Tourmaline may be present in large quantities in exo-contact zones where granite-derived B-rich fluids reached reactive country rock. The occurrence of tourmaline in the slate mantle and their quartz-tourmaline veins are related to the contact metamorphic alteration of the slate. Tourmaline here is generally fine crystalline, with diverse composition, but in stark contrast to the chemistry of the tourmaline in the granite. The progressive crystallization of tourmaline resulted in a sudden increase in the dravite component as the magnesium of the slate became available. As the Al content increased and more Al incorporated at the Y site, the occupation of alkaline metals at the X position decreased and the composition of tourmaline shifted mainly towards foitite/magnesio-foitite. In tourmaline-fels of the slate mantle, and hydrothermal quartz-tourmaline veins and breccias, the complex chemical zonation of the tourmalines distinguishes them from the intragranitic tourmaline which disseminated in the granite. The composition of hydrothermal tourmaline is more varied, with more Mg content and lower X-site occupancy; however, microprobe data suggest no or only a small amount of Fe^{3+} content. The host

rocks of the hydrothermal tourmaline represent an open chemical system where most of the fluid components originated from the country rocks, and the granite is the essential source of the magmatic boron. The individual tourmaline crystals of the veins and breccias show an oscillatory zoning, i.e., there is no definite trend in their chemical evolution.

ACKNOWLEDGEMENTS

The authors would like to thank the Mining and Geological Survey of Hungary (Budapest) for providing samples to undertake the research. Special thanks go to Dr. Bálint Péterdi for his help in the sampling. We are grateful to Ms. Délia Debus (University of Miskolc) for making the polished stubs. Both referees, Dr. Edit Király (Mining and Geological Survey of Hungary, Budapest) and Dr. Elemér Pál-Molnár (University of Szeged) are highly acknowledged for their comments and suggestions that greatly helped to improve the manuscript.
The research was carried out at the University of Miskolc, both as part of the "More efficient exploitation and use of subsurface resources" project implemented in the framework of the Thematic Excellence Program funded by the Ministry of Innovation and Technology of Hungary (Grant Contract reg. nr.: NKFIH-846-8/2019) and the project titled as "Developments aimed at increasing social benefits deriving from more efficient exploitation and utilization of domestic subsurface natural resources" supported by the Ministry of Innovation and Technology of Hungary from the National Research, Development and Innovation Fund in line with the Grant Contract issued by the National Research, Development and Innovation Office (Grant Contract reg. nr.: TKP-17-1/PALY-2020).

REFERENCES

Bačík, P. (2015). Cation ordering at octahedral sites in schorl-dravite series tourmalines. *Canadian Mineralogist*, 53: 571–590.

Benard, F., Moutou, P., and Pichavant, M. (1985). Phase relations of tourmaline leucogranites and the significance of tourmaline in silicic magmas. *Journal of Geology*, 93: 271–291.

Benkó, Zs., Molnár, F., Lespinasse, M., and Váczi, T. (2014). Evidence for exhumation of a granite intrusion in a regional extensional stress regime based on coupled microstructural and fluid inclusion plane studies – an example from the Velence Mts., Hungary. *Journal of Structural Geology*, 65: 44–58.

Buda, Gy. (1969). Genesis of the granitoid rocks of the Mecsek and Velence Mountains on the basis of the investigation of the feldspars. *Acta Geologica Academiae Scientiarum Hungaricae*, 13: 131–155.

Buda, Gy. (1974). Investigation of the alkali feldspar polymorphs of the Hungarian granitoid rocks. *Acta Geologica Academiae Scientiarum Hungaricae*, 18: 465–480.

Buda, Gy. (1981). Genesis of the Hungarian granitoid rocks. *Acta Geologica Academiae Scientiarum Hungaricae*, 24: 309–318.

Buda, Gy. (1985). Variszkuszi korú kollíziós granitoidok képződése Magyarország, Ny-Kárpátok és a Központi Cseh (Bohémiai) masszívum granitoidjainak példáin [origin of collision-type Variscan granitoids in Hungary, West-Carpathians and Central Bohemian Pluton]. Unpublished Ph.D. thesis, Hungarian Academy of Sciences, Budapest (in Hungarian).

Buda, Gy. (1993). Enclaves and fayalite-bearing pegmatitic "nests" in the upper part of the granite intrusion of the Velence Mts., Hungary. *Geologica Carpathica*, 44: 143–153.

Buda, Gy., Koller, F., Kovács, J., and Ulrych, J. (2004a). Compositional variation of biotite from Variscan granitoids in Central Europe: a statistical evaluation. *Acta Mineralogica-Petrographica*, 45(1): 21–37.

Buda, Gy., Koller, F., and Ulrych, J. (2004b). Petrochemistry of Variscan granitoids of Central Europe: correlation of Variscan granitoids of the Tisia and Pelsonia Terranes with granitoids of the Moldanubicum, western Carpathian and southern Alps. A review: Part I. *Acta Geologica Hungarica*, 47: 117–138.

Čech, V. I. (1963). About the antagonism between tourmaline and biotite. *Časopis Národního Muzea, Oddil Přírodovědny*, 132: 146–148.

Embey-Isztin, A. (1974). Petrochemistry of the dike-rocks in the Velence Hills (Hungary). *Annales Historico-Naturales Musei Nationalis Hungarici*, 66: 23–32.

Embey-Isztin, A. (1975). Dilatációs és kiszorításos (metaszomatikus) telérek a Velencei-hegységben (Dilatation-injection and replacement dikes in the Velence Hills). *Fragmenta Mineralogica et Palaeontologica*, 6: 43–61 (in Hungarian with English abstract).

Grice, J. D. and Ercit, T. S. (1993). Ordering of Fe and Mg in the tourmaline crystal structure: the correct formula. *Neues Jahrbuch für Mineralogie Abhandlungen*, 165: 245–266.

Guillot, S. and Le Fort, P. (1995). Geochemical constraints on the bimodal origin of High Himalayan leucogranites. *Lithos*, 35: 221–234.

Gyalog, L. (2005a). *Geological map of Hungary. L-34-25 Székesfehérvár. 1:100,000*. Geological Institute of Hungary, Budapest.

Gyalog, L. (2005b). *Geological map of Hungary. L-34-26 Százhalombatta (Ráckeve). 1:100,000*. Geological Institute of Hungary, Budapest.

Gyalog, L. and Horváth, I. (Eds.) (2004). *Geology of the Velence Hills and the Balatonfő*. Geological Institute of Hungary, Budapest, 316 pp.

Hawthorne, F. C. (1996). Structural mechanisms for light-element variations in tourmaline. *Canadian Mineralogist*, 34: 123–132.

Henry, D. J. and Dutrow, B. L. (1996). Metamorphic tourmaline and its petrologic applications. In: Grew, E. S. and Anovitz, L. M. (Eds.), *Boron. Mineralogy, petrology and geochemistry*. Reviews in Mineralogy, 33: 503–557.

Henry, D. J., and Guidotti, C. V. (19850. Tourmaline as a petrogenetic indicator mineral: an example from the staurolite-grade metapelites of NW Maine. *American Mineralogist*, 70: 1–15.

Henry, D. J., Novák, M., Hawthorne, F. C., Ertl, A., Dutrow, B. L., Uher, P., and Pezzotta, F. (2011). Nomenclature of the tourmaline-supergroup minerals. *American Mineralogist*, 96: 895–913.

Horváth, I., Ódor, L., and Kovács, L. Ó. (1989). A velencei-hegységi gránit metallogéniai sajátosságai (Metallogenic features of the Velence Mts. granitoids). *Annual Report of the Hungarian Geological Survey for the year 1987*, pp. 349–365 (in Hungarian with English abstract).

Hraško, Ľ., Bezák, V., and Molák, B. (1997). Postorogenic peraluminous two-mica granites and granite-porphyries in the Kohút zone of the Veporicum Unit (Klenovec-Zlatno area). *Mineralia Slovaca*, 29: 113–135 (in Slovak with English abstract).

Jantsky, B. (1957). A Velencei-hegység földtana (Géologie de la Montagne de Velence). *Geologica Hungarica – Series Geologica*, 10: 1–170 (in Hungarian with French and Russian summaries).

Jolliff, B. L., Papike, J. J., and Shearer, C. K. (1986). Tourmaline as a recorder of pegmatite evolution: Bob Ingersoll pegmatite, Black Hills, South Dakota. *American Mineralogist*, 71: 472–500.

London, D. (1999). Stability of tourmaline in peraluminous granite systems: the boron cycle from anatexis to hydrothermal aureoles. *European Journal of Mineralogy*, 11: 253–262.

London, D. and Manning, D. A. C. (1995). Chemical variation and significance of tourmaline from Southwest England. *Economic Geology*, 90: 495–519.

London, D., Morgan, G. B., and Wolf, M. B. (1996). Boron in granitic rocks and their contact aureoles. In: Grew, E. S. and Anovitz, L. M. (Eds.), *Boron. Mineralogy, petrology and geochemistry*. Reviews in Mineralogy, 33: 299–330.

Maniar, P. D. and Piccoli, P. M. (1989). Tectonic discrimination of granitoids. *Geological Society of America Bulletin*, 101: 635–643.

Molnár, F. (2004). Characteristics of Variscan and Paleogene fluid mobilization and ore forming processes in the Velence Mts., Hungary: a comparative fluid inclusion study. *Acta Mineralogica-Petrographica*, 45(1): 55–63.

Molnár, F., Török, K., and Jones, P. (1995). Crystallization conditions of pegmatites from the Velence Mts, Western Hungary, on the basis of thermobarometric studies. *Acta Geologica Hungarica*, 38: 57–80.

Nabelek, P. I., Russ-Nabelek, C., and Denison, J. R. (1992). The generation and crystallization conditions of the Proterozoic Harney peak leucogranite, Black Hills, South Dakota, USA: petrologic and geochemical constraints. *Contributions to Mineralogy and Petrology*, 110: 173–191.

Nagy, B. (1967a). A sukorói turmalinos pegmatitelőfordulás ásványkőzettani, geokémiai vizsgálata (Mineralogical, petrographical and geochemical studies on a pegmatite at Sukoró, Velence Mts.). *Annual Report of the Hungarian Geological Survey for the year 1965*, pp. 507–515 (in Hungarian with English abstract).

Nagy, B. (1967b). A velencei-hegységi gránitos kőzetek ásványkőzettani, geokémiai vizsgálata (Mineralogy, petrography and geochemistry of granitic rocks from the Velence Mountains). *Földtani Közlöny*, 97: 423–436 (in Hungarian with English abstract).

Neugebauer, J. (1988). The Variscan plate tectonic evolution: an improved "Iapetus model". *Schweizerische Mineralogische und Petrographische Mitteilungen*, 68: 313–333.

Novák, M., Škoda, R., Filip, J., Macek, I., and Vaculovič, T. (2011). Compositional trends in tourmaline from intragranitic NYF pegmatites of the Třebíč pluton, Czech Republic: an electron microprobe, Mössbauer and LA-ICP-MS study. *Canadian Mineralogist*, 49: 359–380.

Ondrejka, M., Bačík, P., Sobocký, T., Uher, P., Škoda, R., Mikuš, T., Luptáková, J., and Konečný, P. (2018). Minerals of the rhabdophane group and the alunite supergroup in microgranite: products of low-temperature alteration in a highly acidic environment from the Velence Hills, Hungary. *Mineralogical Magazine*, 82: 1277–1300.

Pantó, Gy. (1977). Genetic significance of rare earth elements in the granitoid rocks of Hungary. *Acta Geologica Academiae Scientiarum Hungaricae*, 21: 105–113.

Pesquera, A., Torres-Ruiz, J., García-Casco, A., and Gil-Crespo, P. P. (2013). Evaluating the controls on tourmaline formation in granitic systems: a case study on peraluminous granites from the Central Iberian Zone (CIZ), Western Spain. *Journal of Petrology*, 54: 609–634.

Petrík, I., Broska, I., Bezák, V., and Uher, P. (1995). The Hrončok (Western Carpathians) type granite – a Hercynian A-type granite in shear zone. *Mineralia Slovaca*, 27: 351–364 (in Slovak with English abstract).

Pouchou, J. L. and Pichoir, F. (1985). "PAP" ($\varphi\rho Z$) procedure for improved quantitative microanalysis. In: Armstrong, J. T. (Ed.), *Microbeam analysis*. San Francisco Press, San Francisco, pp. 104–106.

Scaillet, B., Pichavant, M., and Roux, J. (1995) Experimental crystallization of leucogranite magmas. *Journal of Petrology*, 36: 663–705.

Shand, S. J. (1943). The eruptive rocks, 2nd ed. John Wiley, New York. 444 pp.

Szakáll, S., Dill, H. G., and Melcher, F. (2007). Hinsdalit, egy új APS-ásvány a Velencei-hegységből (Nadap, Meleg-hegy) [Hinsdalite, a new APS mineral from Meleg Hill, Nadap (Velence Mountains, Hungary)]. *Acta GGM Debrecina, Geology, Geomorphology, Physical Geography Series*, 2: 33–36 (in Hungarian).

Szakáll, S., Gyalog, L., Kristály, F., Zajzon, N., and Fehér, B. (2014). Ritkaföldfémek a velencei-hegységi granitoidokban és alkáli magmás kőzetekben [Rare earth elements in the granitoids and alkali magmatic rocks of the Velence Mts.]. In: Szakáll, S. (Ed.), *Ritkaföldfémek magyarországi földtani képződményekben* [Rare earth elements in geological formations of Hungary]. CriticEl Monography Series, vol. 5. Milagrossa kft., Miskolc, pp. 67–90 (in Hungarian).

Szakáll, S., Fehér, B., and Tóth, L. (2016). Magyarország ásványai [Minerals of Hungary]. GeoLitera, Szeged, 526 pp. (in Hungarian).

Uher, P. and Broska, I. (1994). The Velence Mts. granitic rocks: geochemistry, mineralogy and comparison to Variscan Western Carpathian granitoids. *Acta Geologica Hungarica*, 37: 45–66.

Uher, P. and Broska, I. (1996). Post-orogenic Permian granitic rocks in the Western Carpathian-Pannonian area: geochemistry, mineralogy and evolution. *Geologica Carpathica*, 47: 311–321.

Uher, P. and Gregor, T. (1992). The Turčok granite: product of post-orogenic A-type magmatism? *Mineralia Slovaca*, 24: 301–304 (in Slovak with English abstract).

Uher, P. and Ondrejka, M. (2009). The Velence granites, Transdanubic Superunit: a product of Permian A-type magmatism and Alpine overprint (results of zircon SHRIMP and monazite EMPA dating). HUNTEK 2009, Proceedings of the 7th Meeting of the Central European Tectonic Studies Group (CETeG) and

14th Meeting of the Czech Tectonic Studies Group (CTS) at Pécs, Hungary. Abstracts, p. 32.

Uher, P., Marschalko, R., Martiny, E., Puškelová, Ľ., Streško, V., Toman, B., and Walzel, E. (1994). Geochemical characterization of granitic rock pebbles from Cretaceous to Paleogene flysch of the Pieniny Klippen belt. *Geologica Carpathica*, 45: 171–183.

van Hinsberg, V. J., Henry, D. J., and Marschall, H. R. (2011). Tourmaline: an ideal indicator of its host environment. *Canadian Mineralogist*, 49: 1–16.

Vendl, A. (1914). A Velencei hegység geológiai és petrografiai viszonyai [Geological and petrographical conditions of the Velence Mountains]. *Magyar Királyi Földtani Intézet Évkönyve*, 22(1): 1–169 (in Hungarian).

Vendl, M. (1923). Újabb adatok a Velenczei hegység kőzeteinek ismeretéhez [New data on the knowledge of the rocks of the Velence Mountains]. *Annales Musei Nationalis Hungarici*, 20: 81–84 (in Hungarian).

Wise, M. (1999). Characterization and classification of NYF-type pegmatites. *Canadian Mineralogist*, 37: 802–803.

Wolf, M. B. and London, D. (1997). Boron in granitic magmas: stability of tourmaline in equilibrium with biotite and cordierite. *Contributions to Mineralogy and Petrology*, 130: 12–30.

Zajzon, N., Szakáll, S., Kristály, F., Váczi, T., and Fehér, B. (2015). Gadolinite-bearing NYF-type pegmatite from Sukoró, Velence Hills, Hungary. *Acta Mineralogica-Petrographica*, *Abstract Series*, 9, p. 75.